Department of Electrical
and
Computer Systems Engineering

Technical Report
MECSE-8-2005

Photonic Fiber Ring Lasers: Stability, Harmonic Detuning, Temporal Diffraction and Multi-wavelength Generation

Le Nguyen Binh

MONASH
UNIVERSITY

PHOTONIC FIBER RING LASERS[1]:

STABILITY, HARMONIC DETUNING, TEMPORAL DIFFRACTION AND MULTI-WAVELENGTTH GENERATION

Le Nguyen Binh
Department of Electrical and Computer Systems Engineering
Monash University, Clayton Victoria 3168 Australia

SUMMARY

This report describes a detailed account of the design, construction and characterisation of photonic fiber ring lasers: the harmonic and regenerative mode locked type for 10 and 40 G-pules/sec., harmonic detuning type for up to 200 G-pulses/sec., the harmonic repetition multiplication via temporal diffraction, and the multi—wavelength type.

Mode-locked (ML) laser structures consist of in-line optical fiber amplifiers, guided-wave optical intensity Mach-Zehnder interferometric modulator (MZIM) and associate optics to form the structure of a ring resonator for the generation of photonkic pulse trains of several GHz rep-rate with pulse duration in order of ps or sub-ps. This rate has been extended further to a few hundreds Giga-pulses/sec. by using the temporal diffraction Talbot effect that eliminates the bandwidth limitation of the optical modulator incorporated in the laser ring.

*A mode-locked laser operating at 10 GHz repetition rate has been designed, constructed and tested. The laser generates optical pulse train of 4.5 ps pulse width when the modulator is biased at the phase quadrature quiescent region. Preliminary experiment of a 40 GHz repetition rate mode-locked laser has also been demonstrated. We have achieved long term stability of amplitude and phase noise that indicates that the optical pulse source can produce an error-free PRBS pattern in a self-locking mode for more than 20 hours, **the most stable photonic fiber ring laser reported to date.***

The rep-rate of the mode locked fibre ring laser is demonstrated up to 200 Gpulses/sec. using harmonic detuning mechanism in a ring laser. In this system, we investigate the system behaviour of rational harmonic mode-locking in the fiber ring laser using phase plane technique of the nonlinear control engineering. Furthermore, we examine the harmonic distortion contribution to this system performance. We also demonstrate 660x and 1230x repetition rate multiplications on 100MHz pulse train

---

MONASH UNIVERSITY

*generated from an active harmonically mode-locked fiber ring laser, hence achieve 66 GHz and 123 GHz pulse operations, which is **the highest rational harmonic order reported to date***.

*The system behavior of group velocity dispersion (GVD) repetition rate multiplication in optical communication systems is also demonstrated. **The stability and the transient response of the multiplied pulses are studied using the phase plane technique of nonlinear control engineering.** We also demonstrated four times repetition rate multiplication on 10 G-pules/s pulse train generated from the active harmonically mode-locked fiber ring laser, hence achieving 40Gpulses/s pulse train by using fiber GVD effect. It has been found that the stability of the GVD multiplied pulse train, based on the phase plane analysis is hardly achievable even under the perfect multiplication conditions. Furthermore, uneven pulse amplitude distribution is observed in the multiplied pulse train. In addition to that, the influences of the filter bandwidth in the laser cavity, nonlinear effect and the noise performance are also studied in our analyses.*

*Finally, we present the theoretical development and demonstration of **a multi-wavelength optically amplifier fiber ring laser** using an all-polarization-maintaining fiber (PMF) Sagnac loop. The Sagnac loop simply consists of a PMF coupler and a segment of stress-induced PMF, with a single-polarization coupling point in the loop. The Sagnac loop is shown to be a stable comb filter with equal frequency period which determines the possible output power spectrum of the fiber ring laser. The number of output lasing wavelengths is obtained by adjusting the polarization state of the light in the unidirectional ring cavity by means of a polarization controller.*

Multi-wavelength ultra-short-width ultra-high rep-rate photonic generators will be proposed and reported in the near future, by combining the principles of the above photonic fiber ring lasers

MONASH
U N I V E R S I T Y

TABLE OF CONTENTS

MONASH
U N I V E R S I T Y

TABLE OF FIGURES

MONASH UNIVERSITY

MONASH
U N I V E R S I T Y

1 INTRODUCTION

Generation of ultra-short optical pulses with multiple gigabits repetition rate is critical for ultra-high bit rate optical communications, particularly for the next generation of terabits/sec. optical fibers systems. As the demand for the bandwidth of the optical communication systems increases, the generation of short pulses with ultra-high repetition rate becomes increasingly important in the coming decades.

The mode locked fibers laser offers a potential source of such pulse train. Although the generation of ultra-short pulses by mode locking of a multi-modal ring laser is well known, the applications of such short pulse trains in multi-gigabits/sec optical communications challenges its designers on its stability and spectral properties. Recent reports on the generation of short pulse trains at repetition rates in order of 40 Gb/s, possibly higher in the near future[1], motivates us to design and experiment with these sources in order to evaluate whether they can be employed in practical optical communications systems.

Further the interest of multiplexed transmission at 160 Gb/s and higher in the foreseeable future, requires us to experiment with optical pulse source having a short pulse duration and high repetition rates. This report describes laboratory experiments of a mode-locked fibers ring laser (MLFRL), initially with a repetition rate of 10 GHz and preliminary results of higher multiple repetition rates up to 40 GHz. The mode locked ring lasers reported hereunder adopt an active mode locking scheme whereby partial optical power of the output optical waves is detected, filtered and a clock signal is recovered at the desired repetition rate. It is then used as a RF drive signal to the intensity modulator incorporated in the ring laser. A brief description on the principle of operation of the MLFRL is given in the next section followed by a description of the mode-locked laser experimental set up and characterisation.

Active mode-locked fiber lasers remain as a potential candidate for the generation of such pulse trains. However, the pulse repetition rate is often limited by the bandwidth of the modulator used or the radiofrequency (RF) oscillator that generates the modulation signal. Hence, some techniques have been proposed to increase the repetition frequency of the generated pulse trains. Rational harmonic mode-locking is widely used to increase the system repetition frequency [1-3]. 40GHz repetition frequency has been obtained with 4th order rational harmonic mode locking at 10GHz base band modulation frequency [2]. [3] has reported 22nd order rational harmonic detuning in the active mode-locked fiber laser, with 1GHz base frequency, leading to 22GHz pulse operation. This technique is simple and achieved by applying a slight deviated frequency from the multiple of fundamental cavity frequency. Nevertheless, it is well known that it suffers from inherent pulse amplitude instability as well as poor long-term stability. Therefore, pulse amplitude equalization techniques are often applied to achieve better system performance [3], [4, 5].

MONASH
UNIVERSITY

Other than this rational harmonic detuning, there are some other techniques have been reported and used to achieve the same objective. Fractional temporal Talbot based repetition rate multiplication technique [6, 7] uses the interference effect between the dispersed pulses to achieve the repetition rate multiplication. The essential element of this technique is the dispersive medium, such as linearly chirped fiber grating (LCFG) [6, 8] and dispersive fiber [9-11]. Intracavity optical filtering [12, 13] uses modulators and a high finesse Fabry-Perot filter (FFP) within the laser cavity to achieve higher repetition rate by filtering out certain lasing modes in the mode-locked laser. Other techniques used in repetition rate multiplication include higher order FM mode-locking [14], optical time domain multiplexing [15], etc.

The stability of high repetition rate pulse train generated is one of the main concerns for practical multi-Giga bits/sec optical communications system. Qualitatively, a laser pulse source is considered as stable if it is operating at a state where any perturbations or deviations from this operating point is not increased but suppressed. Conventionally the stability analyses of such laser systems are based on the linear behavior of the laser in which we can analytically analyze the system behavior in both time and frequency domains. However, when the mode-locked fiber laser is operating under nonlinear regime, none of these standard approaches can be used, since direct solution of nonlinear different equation is generally impossible, hence frequency domain transformation is not applicable. Some inherent nonlinearities in the fiber laser may affect its stability and performance, such as the saturation of the embedded gain medium, non-quadrature biasing of the modulator, nonlinearities in the fiber, etc., hence, nonlinear stability approach should be used in any laser stability analysis.

In section 2, we focus on the stability and transient analyses of the rational harmonic mode-locking in the fiber ring laser system using phase plane method, which is commonly used in nonlinear control system. This technique has been previously used in [11] to study the system performance of the fractional temporal Talbot repetition rate multiplication systems. It has been shown that it is an attractive tool in system behavior analysis. However, it has not been used in the rational harmonic mode-locking fiber laser system. In Section 3.1, the rational harmonic detuning technique is briefly discussed. Section 3.2 describes the experimental setup for the repetition rate multiplication used. Section 3.3 investigates the dynamic behavior of the phase plane of the fiber laser system, followed by some simulation results. Section 3.4 presents and discusses the results obtained from the experiment and simulation. Finally, some concluding remarks and possible future developments for this type of ring laser are given.

Rational harmonic detuning [3, 16] is achieved by applying a slight deviated frequency from the multiple of fundamental cavity frequency. 40Ghz repetition frequency has been obtained by [3] using 10GHz base band modulation frequency with 4th order rational harmonic mode locking. This technique is simple in nature. However, this technique suffers from inherent

MONASH
UNIVERSITY

pulse amplitude instability, which includes both amplitude noise and inequality in pulse amplitude, furthermore, it gives poor long-term stability. Hence, pulse amplitude equalization techniques are often applied to achieve better system performance [2], [4, 5]. Fractional temporal Talbot based repetition rate multiplication technique [4-8] uses the interference effect between the dispersed pulses to achieve the repetition rate multiplication. The essential element of this technique is the dispersive medium, such as linearly chirped fiber grating (LCFG) [8, 16] and single mode fiber [8, 9]. This technique will be discussed further in Section II. Intracavity optical filtering [13, 14] uses modulators and a high finesse Fabry-Perot filter (FFP) within the laser cavity to achieve higher repetition rate by filtering out certain lasing modes in the mode-locked laser. Other techniques used in repetition rate multiplication include higher order FM mode-locking [13], optical time domain multiplexing, etc.

The stability of high repetition rate pulse train generated is one of the main concerns for practical multi-Giga bits/sec optical communications system. Qualitatively, a laser pulse source is considered as stable if it is operating at a state where any perturbations or deviations from this operating point is not increased but suppressed. Conventionally the stability analyses of such laser systems are based on the linear behavior of the laser in which we can analytically analyze the system behavior in both time and frequency domains. However, when the mode-locked fiber laser is operating under nonlinear regime, none of these standard approaches can be used, since direct solution of nonlinear different equation is generally impossible, hence frequency domain transformation is not applicable.

Although Talbot based repetition rate multiplication systems are based on the linear behavior of the laser, there are still some inherent nonlinearities affecting its stability, such as the saturation of the embedded gain medium, non-quadrature biasing of the modulator, nonlinearities in the fiber, etc., hence, nonlinear stability approach must be adopted.

In Section 4, we focus on the stability and transient analyses of the grou-velocity-dispersion (GVD) multiplied pulse train using the phase plane analysis of nonlinear control analytical technique [2]. This is the first time, to the best of our knowledge that the phase plane analysis is being used to study the stability and transient performances of the GVD repetition rate multiplication systems. In Section 4.1, the GVD repetition rate multiplication technique is briefly given. Section 4.2 describes the experimental setup for the repetition rate multiplication. Section 4.3 nvestigates the dynamic behavior of the phase plane of GVD multiplication system, followed by some simulation results. Section 4.4 presents and discusses the results obtained from the experiment. Finally, some concluding remarks and possible future developments for this type of lasers are given

Due to the enormous practical applications in components testing and wavelength division multiplexing (WDM) networks and considering that the complexity and cost of optical sources will increase as the number of wavelength channels increases, multi-wavelength optical

sources capable of generating a large number of wavelengths have been an area of strong and continuing worldwide research interest. Erbium-doped fiber lasers operating in the 1550-nm window are widely used in WDM systems, fiber-optic sensor systems, and photonic true-time delay beam forming systems [17]-[18]. Among these different types of fiber lasers, unidirectional traveling-wave ring lasers have been studied extensively in recent years due to several advantages such as elimination of back scattering and spatial hole-burning effects. Several types of optical filters such as fiber Bragg gratings (FBGs) [19], [20], Fabry-Perot filters [21], multi-mode filters [22], and high-birefringence fibers [23] have been used in the construction of multi-wavelength fiber ring lasers . Multi-wavelength fiber lasers using FBGs as wavelength-selective filters will require a large number of individual FBGs to be written on one single segment of fiber depending on the number of lasing wavelengths to be generated. This type of fiber laser has high insertion loss and is costly due to a large number of phase masks required to fabricate the FBGs.

The Sagnac loop simply consists of a PMF coupler and a segment of stress-induced PMF, with a single-polarization coupling point in the loop. The Sagnac loop is shown to be a stable comb filter with equal frequency period which determines the possible output power spectrum of the fiber ring laser. The number of output lasing wavelengths is obtained by adjusting the polarization state of the light in the unidirectional ring cavity by means of a polarization controller.

Sagnac fiber interferometers have several applications, such as gyroscopes, magnetic field sensors, and secure optical communications. A Sagnac loop filter simply consists of a fiber coupler whose two ends are spliced to the two ends of a segment of optical fiber (see Fig. 1(a)). The Sagnac loop can function as a reflector or periodic filter depending on the birefringence with the fiber loop. The Sagnac loop is simply a reflector when there is no birefringence in the fiber loop. Due to the frequency dependence of the coupler, the coupler acts as a reflector when its coupling coefficient is 50% and as a partial reflector for other values of coupling coefficient. The Sagnac loop as a reflector has been used in the fabrication of fiber laser with a linear cavity [24]. Also the Sagnac loop can function as a periodic filter when there is some birefringence induced in the loop [25, 26]. Compared with a Mach-Zehnder interferometer, the Sagnac loop filter is more robust against environmental changes because it is a two-beam interferometer with one common path. However, the Sagnac filter may not operate stably when only standard single-mode fibers are used to form the coupler and the loop. This is because that the small fiber core imperfection, external stress, bending, twisting and temperature variation may cause the spliced sections of the coupler and the loop to behave as a birefringent media whose birefringence changes randomly with time. It should be noted that references [25] and [26] do not provide a complete theoretical basis of the effect of the linear birefringence on the performance of the Sagnac filter which is presented in this section. This kind of birefringent loop filter has been placed inside the linear cavity of a fiber

laser with a polarization controller inside the loop, because the coupler was made of standard single-mode fiber [27].

In this section, we present a theoretical analysis and implementation of a multi-wavelength fiber ring laser (MWFRL) with a Sagnac PMF loop filter. It is shown that when a single-polarization coupling point is formed by the stress-induced PMF loop, the fiber laser can provide stable generation of multiple lasing wavelengths with equal wavelength spacing. Section 5.1 presents the theory of the Sagnac PMF loop filter, which consists of a PMF coupler (instead of a standard single-mode fiber coupler used in previous works as described above) and a segment of PMF. Section 5.2 presents the experimental results and discussion. Concluding remarks are given in Section 5.3.

2   ULTRA-HIGH REP-RATE FIBER MODE-LOCKED LASERS

This section gives a detailed account of the design, construction and characterisation of a mode-locked (ML) fibers ring laser. The ML laser structure employs in-line optical fibers amplifiers, a guided-wave optical intensity Mach-Zehnder interferometric modulator (MZIM) and associate optics to form a ring resonator structure generating optical pulse trains of several GHz repetition rate with pulse duration in order of pico-seconds. Long term stability of amplitude and phase noise has been achieved that indicates that the optical pulse source can produce an error-free PRBS pattern in a self-locking mode for more than 20 hours. A mode-locked laser operating at 10 GHz repetition rate has been designed, constructed, tested and packaged. The laser generates optical pulse train of 4.5 ps pulse width when the modulator is biased at the phase quadrature quiescent region. Preliminary experiment of a 40 GHz repetition rate mode-locked laser has also been demonstrated. Although it is still unstable in long term, without an O/E feedback loop, optical pulse trains have been observed.

2.1   Mode-locking techniques and conditions for generation of transform limited pulses from a mode locked laser

1.2.1   Schematic structure of MLRL

Figure 1 and Figure 2 show the composition of a MLRL without and with feedback loop used in this study respectively. It consists principally, for a non-feedback ring, an optical close loop with an optical gain medium, an optical modulator (intensity or phase type) an optical fibers coupler and associated optics. An O/E feedback loop detecting and repetition-rate signal and generating RF sinusoidal waves to electro-optically drive the intensity modulator is necessary for the regenerative configuration as shown in Figure 2.

MONASH
UNIVERSITY
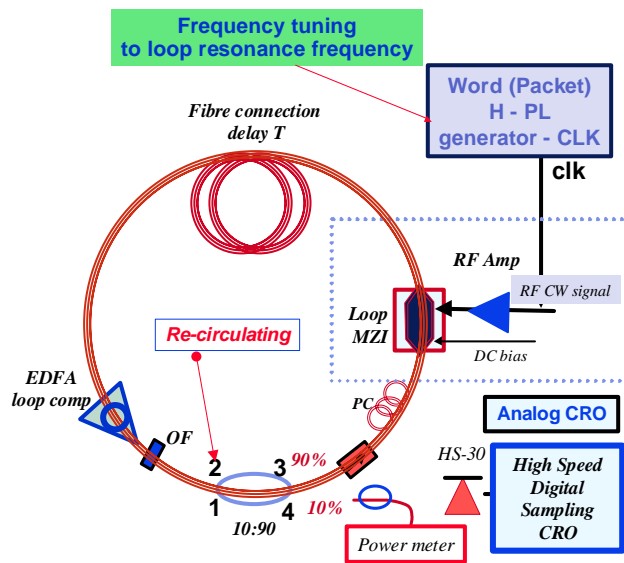
Figure 1 *Schematic arrangement of a mode-locked ring laser without the active feedback control.*
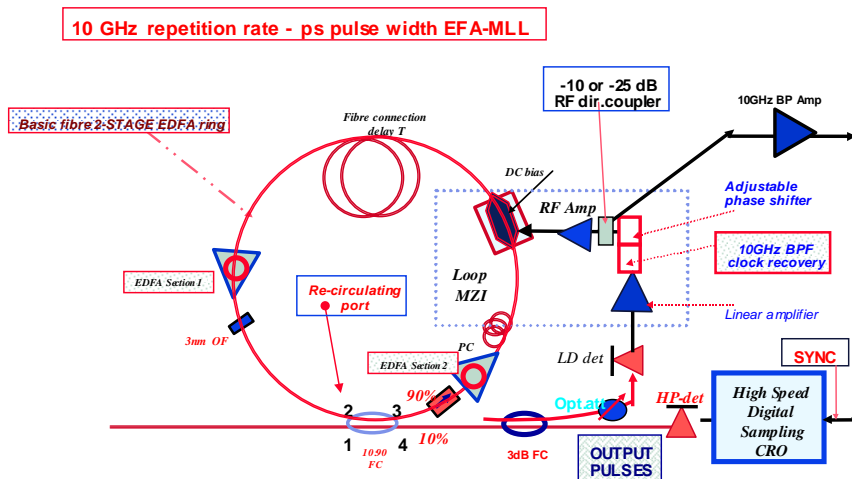
Figure 2 *Schematic arrangement of a mode-locked ring laser with an O/E-RF electronic active feedback loop*

1.2.2   Mode-locking conditions

The basic conditions for MLRL to operate in pulse oscillation are:

MONASH
UNIVERSITY

For non-feedback optical mode-locking

Condition 1: The total optical loop gain must be greater than unity when the modulator is ON-state, i.e. when the optical waves transmitting through the MZIM is propagating in phase[28];

Condition 2: The optical lightwaves must be depleted when the optical modulator is in the OFF-state, i.e. when the lightwaves of the two branches of the MZIM is out of phase or in destructive interference mode[28];

Condition 3: The frequency repetition rate at a locking state must be a multiple number of the fundamental ring resonant frequency[29].

For optical-RF feedback mode locking - Regenerative mode-locking

Condition 4: Under an O/E-RF feedback to control modulation of the intensity modulator the optical noise at the output of the laser must be significantly greater than that of the electronic noise for the start-up of the mode locking and lasing. In other words the loop gain of the optical-electronic feedback loop must be greater than unity.

Thus it is necessary that the EDF amplifiers are operated in saturation mode and the total average optical power of the lightwaves circulating in the loop must be sufficiently adequate for the detection at the photo-detector and electronic preamplifier. Under this condition the optical quantum shot noise dominates the electronic shot noise.

1.2.3   Factors influencing the design and performance of mode-locking and generation of optical pulse train

The locking frequency is a multiple of the fundamental harmonic frequency of the ring defined as the inverse of the travelling time around the loop and is given by

$$f_{RF} = \frac{Nc}{n_{eff}L}$$

(1)

where f_{RF} is the RF frequency required for locking and the required generation rate, N is an integer and indicates mode number order, c is the velocity of light in vacuum, n_{eff} is effective index of the guided propagating mode and L is loop length including that of the optical amplifiers.

Under the requirement of the OC-192 standard bit rate the locking frequency must be in the region of 9.95 Giga-pulses per second. That is the laser must be locked to a very high order of the fundamental loop frequency that is in the region of 1 MHz to 10 MHz depending on the

MONASH
UNIVERSITY

total ring length. For an optical ring of length about 30 metres and a pulse repetition rate of 10 GHz, the locking occurs on approximately the 1400th harmonic mode.

It is noted also that the effective refractive index n can be varied in different sections of the optical components forming the laser ring. Furthermore the two polarised states of propagating lightwaves in the ring, if the fibers is not a polarisation maintaining type, would form two simultaneously propagating rings, and they could interfere or hop between these dual polarised rings.

The pulse width, denoted as $\Delta\tau$ of the generated optical pulse trains can be found to be given by[30]

$$\Delta\tau = 0.45 \left(\frac{\alpha_t G_t}{\Delta_m} \right)^{1/4} \frac{1}{(f_{RF}\Delta\upsilon)^{1/2}}$$

(2)

with $\alpha_t\Gamma_t$ is the round trip gain coefficient as a product of all the loss and gain coefficients of all optical components including their corresponding fluctuation factor, Δ_m is the modulation index and υ is the overall optical bandwidth (in units of Hz) of the laser.

Hence the modulation index and the bandwidth of the optical filter influence the generated pulse width of the pulse train. However the optical characteristics of the optical filters and optical gain must be flattened over the optical bandwidth of the transform limit for which a transform limited pulse must satisfy, for a sech[2] pulse intensity profile, the relationship

$$\Delta\tau\Delta\upsilon = 0.315$$

(3)

Similarly, for Gaussian pulse shape the constant becomes 0.441.

The fluctuation of the gain or loss coefficients over the optical flattened region can also influence the generated optical pulse width and mode locking condition.

In the case for regenerative mode-locking case as illustrated in Figure 2, the optical output intensity is split and opto-electronically (O/E) detected, we must consider the sensitivity and noises generated at the photo-detector (PD). Two major sources of noises are generated at the in put of the PD, firstly the optical quantum shot noises generated by the detection of the optical pulse trains and the random thermal electronic noises of the small signal electronic amplifier following the detector. Usually the electronic amplifier would have a 50 Ω equivalent input resistance R referred to the input of the optical preamplifier as evaluated at the operating repetition frequency, this gives a thermal noise spectral density of

MONASH
UNIVERSITY

$$S_R = \frac{4kT}{R}$$

A^2/Hz   (4)

with k the Boltzmann's constant. This equals to 3.312 x 10^{-22} A^2/Hz at 300 ^{o}K. Depending on the electronic bandwidth $B_{e\,of}$ the electronic pre-amplifier, i.e. wideband or narrow band type, the total equivalent electronic noise (square of noise 'current') is given by, $i_{NT}^2 = S_R B_e$. Under the worst case when a wide-band amplifier of a 3-dB electrical bandwidth of 10 GHz, the equivalent electronic noise at the input of the electronic amplifier is 3.312 x 10^{-11} A^2, ie. an equivalent noise current of 5.755 μA is present at the input of the 'clock' recovery circuit. If a narrow band-pass amplifier of 50 MHz 3-dB bandwidth centred at 10 GHz is employed this equivalent electronic noise current is 0.181 μA.

Now considering the total quantum shot noise generated at the input of the 'clock' recovery circuit, suppose that a 1.0 mW (or 0 dBm) average optical power is generated at the output of the MLRL, then a quantum shot noise[2] of approximately 2.56 x 10^{-22} A^2 /Hz (ie. an equivalent electronic noise current of 16 nA) is present at the input of the clock recovery circuit. This quantum shot noise current is substantially smaller than that of the electronic noise.

In order for the detected signal at the optical receiver incorporated in the 'clock' recovery circuit to generate a high signal-to-noise ratio the optical average power of the generated pulse trains must be high, at least at a ratio of 10. We estimate that this optical power must be at least 0 dBm at the PD in order for the MLRL to lock efficiently to generate a stable pulse train.

Given that a 10% fibers coupler is used at the optical output and an estimate optical loss of about 12 dB due to coupling, connector loss and attenuation of all optical components employed in the ring, the total optical power generated by the amplifiers must be about 30 dBm. To achieve this we employ two EDF amplifiers of 16.5 dBm output power each positioned before and after the optical coupler, one is used to compensate for the optical losses and one for generating sufficient optical gain and power to dominate the electronic noise in the regenerative loop.

2.2   Experimental set-up and results

The experimental set ups for MLL and RMLL are as shown, again, in Figure 1 and Figure 2. Associate equipment used for monitoring of the mode locking and measurement of the lasers are also included. However we note the followings:

M O N A S H
U N I V E R S I T Y

- In order to lock the lasing mode of the MLL to a certain repetition rate or multiple harmonic of the fundamental ring frequency, a synthesiser is required to generate the required sinusoidal waves for modulating the optical intensity modulator and tuned to a harmonic of the cavity fundamental frequency.

- A signal must be created for the purpose of triggering the digital oscilloscope to observe the locking of the detected optical pulse train. For the HP-54118A amplitude of this signal must be > 200 mV. This is also critical for the RMLL set up as the RF signal detected and phase locked via the clock recovery circuitry must be spit to generate this triggering signal.

Typical experimental procedures are:

- After the connection of all optical components with the ring path broken, ideally at the output of the fibers coupler, a CW optical source can be used to inject optical waves at a specific wavelength to monitor the optical loss of the ring;

- Close the optical ring and monitor the average optical power at the output of the 90:10 fibers coupler and hence estimate the optical power available at the PD is about -3 dBm after a 50:50 fibers coupler;

- Determine whether an optical amplifier is required for detecting the optical pulse train or whether this optical power is sufficient for O/E RF feedback condition as stated above;

- Set the biasing condition and hence the bias voltage of the optical modulator

- Tune the synthesiser or the electrical phase to synchronise the generation and locking of the optical pulse train.

The following results are obtained:

- The optical pulse train generated at the output of the MLL or RMML. Experimental set up is shown in *Figure 3*;

- Synthesised modulating sinusoidal waveforms can be monitored as shown in *Figure 5* and *Figure 6* and *Figure 7*. *Figure 5* illustrates the mode locking of a MLL operating at around 2 GHz repetition rate with the modulator driven from a pattern generator while in *Figure 6* and *Figure 7* show the sinusoidal waveforms generating when the MLRL is operating at the self-mode-locking state.

- The interference of other super-modes of the MLL without RF feedback for self locking is indicated in *Figure 5*;

---

[2] by using the relationship of the quantum noise spectral density of $2qRP_{av}$ with P_{av} the average optical

MONASH
U N I V E R S I T Y

- Observed optical spectrum (not available in electronic form);

- Electrical spectrum of the generated pulse trains was observed showing a -70dB super-mode suppression under the locked state of the regenerative MLRL;

- Figure *Figure 6* and *Figure 8* show that the regenerative MLRL can be operating under the cases when the modulator is biased either at the positive or at the negative going slope of the optical transfer characteristics of the Mach-Zehnder modulator;

- Optical pulse width is measured using an optical auto-correlator (slow or fast scan mode). Typical pulse width obtained with the slow scan auto-correlator is shown in *Figure 10*. Minimum pulse duration obtained was 4.5 ps with a time-bandwidth product of about 3.8 showing that the generated pulse is near transform limited;

- BER measurement was used to monitor the stability of the regenerative MLRL. The BER error detector was then programmed to detect all '1' at the decision level at a tuned amplitude level and phase delay. The clock source used is that produced by the laser itself. This set up is shown in *Figure 4* and an error-free has been achieved for over 20 hours. The O/Eally detected waveform of the output pulse train for testing the BER shown in *Figure 9* after 20 hours operation, the recorded waveform is obtained under infinite persistence mode of the digital oscilloscope;

- A drift of clock frequency of about 20 kHz over one hour in open laboratory environment is observed. This is acceptable for a 10 GHz repetition rate.

- The 'clock' recovered waveforms were also monitored at the initial locked state and after the long-term test as shown in *Figure 6* and *Figure 7* respectively. *Figure 7* obtained under the infinite persistence mode of the digital oscilloscope;

We note the following factors which are related to the above measurements (*Figure 5* to *Figure 7*):

- All the above measurements have been conducted with two distributed optical amplifiers (GTi EDF optical amplifiers) driven at 180 mA and a specified output optical power of 16.5 dBm.

- Optical pulse trains are detected with 34 GHz 3dB bandwidth HP pin detector directly coupled to the digital oscilloscope without using any optical pre-amplifier.

power, q the electronic charge and *R* the responsivity of the detector.
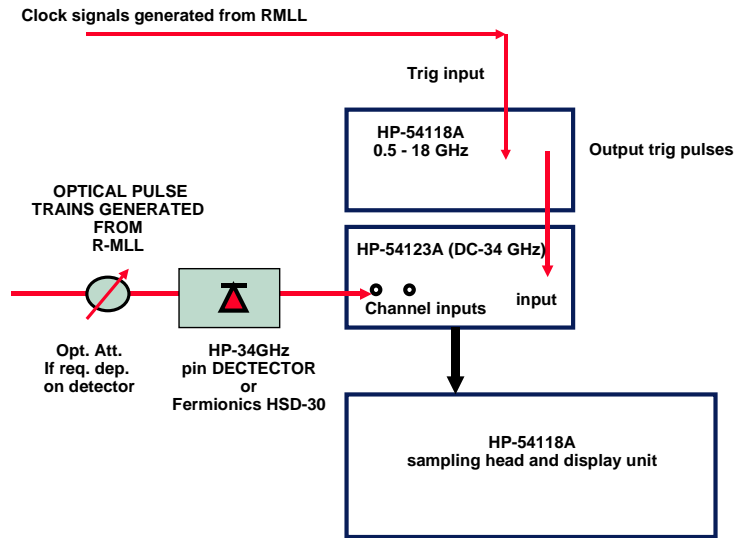
Figure 3 Experimental set up for monitoring the locking of the photonic pulse train.
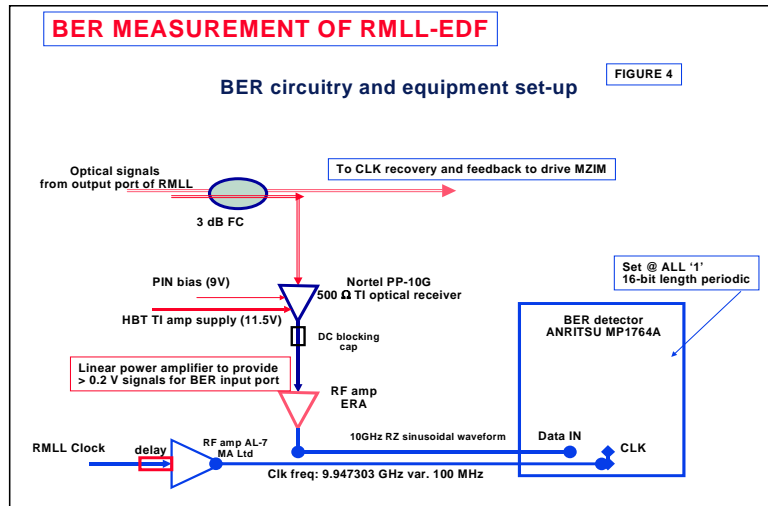
Figure 4 Experimental set up for monitoring the BER of the photonic pulse train.

MONASH
UNIVERSITY
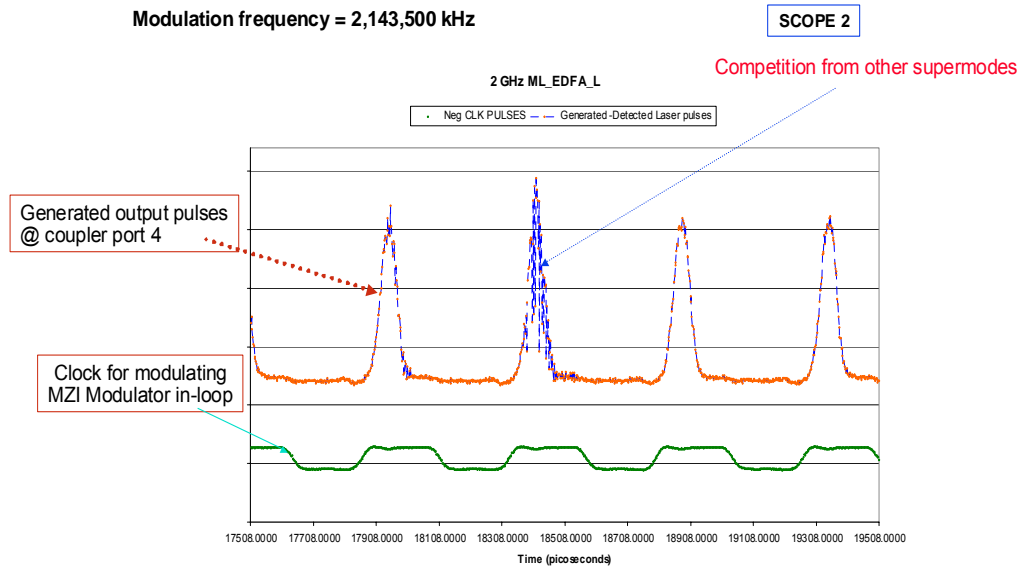
Figure 5 Detected pulse train at the MLRL output tested at a multiple frequency in the range of 2 GHz repetition frequency.
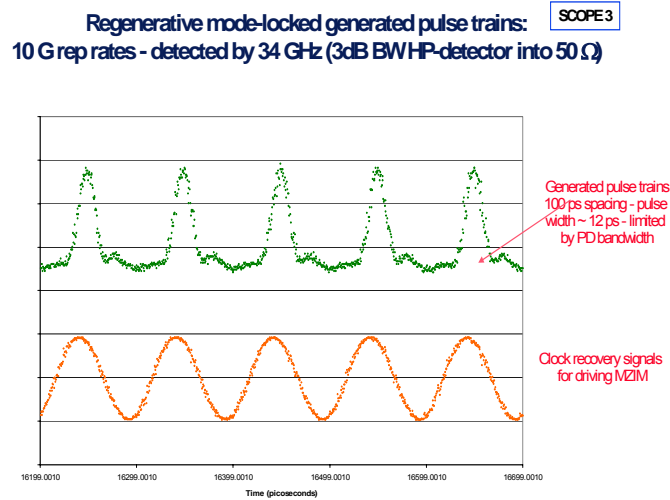
Figure 6 Output pulse trains of the regenerative MLRL and the RF signals as recovered for modulating the MZIM for self-locking
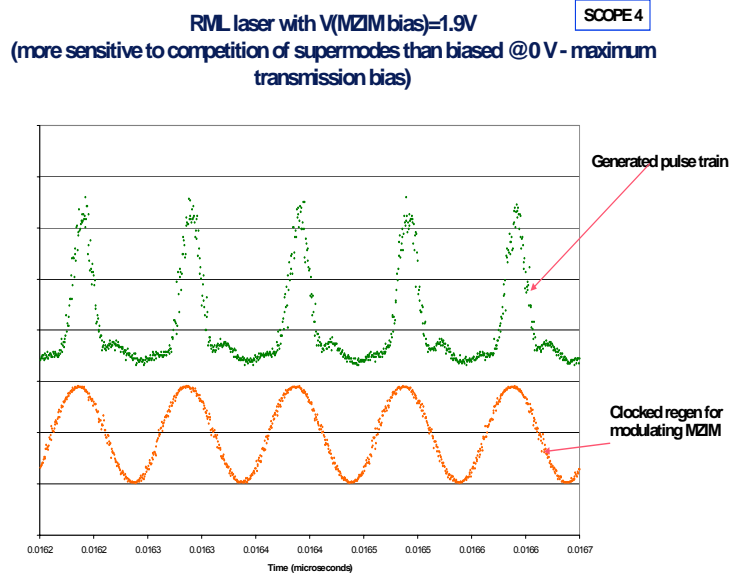
Figure 7 Detected output pulse trains of the regenerative MLRL and recovered clock signal when the MZIM is biased at a negative going slope of the operating characteristics of the modulator
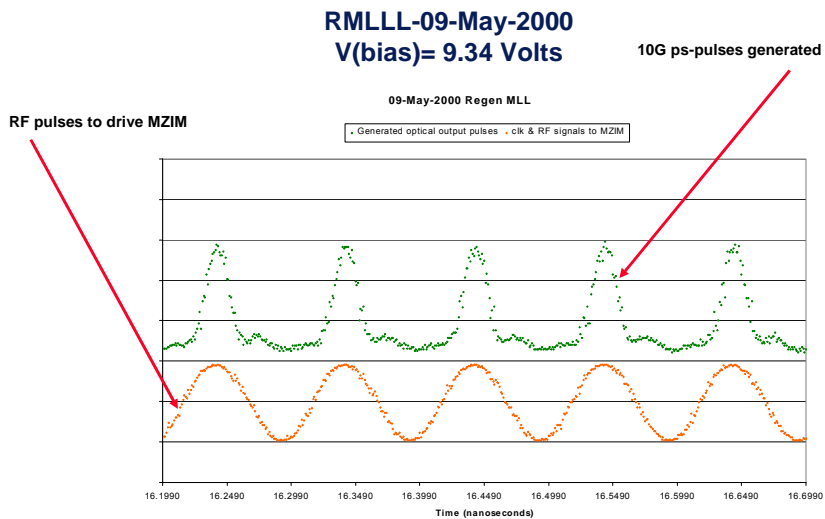
Figure 8 Output pulse trains and clock recovered signals of the 10 G regenerative MLRL when the modulator is biased at the positive going slope of the modulator operating transfer curve

MONASH
UNIVERSITY

BER measurement

BER=0 x 10-15 measured for over 20 hours -
RF (CLK) frequency varied from 9.954 to 9.952 GHz gradually over measurement period

BER measurement - clock signal - infinite persistence

Figure 9 BER measurement – O/E detected signals from the generated output pulse trains for BER test set measurement. The waveform is obtained after 20 hours persistence.

Auto-correlated pulse
V(bias) = 1.55 volt - phase quadrature neg slope
FWHM $\Delta\tau$ = 4.48 ps
autocorrelator set thumbwheel 6 and 0 (100ps range @10ps/s delay rate)

Figure 10 Auto-correlation trace of output pulse trains of 9.95 GHz regenerative MLRL

2.3   40 GHz regenerative mode-locked laser

Following our initial success of the construction and testing of a regenerative MLRL at 40 GHz repetition rate regenerative mode locked laser was constructed. The schematic arrangement of the 40G regenerative MLRL is shown in *Figure 11*. Initial observation of the locking and

© 2005 Le Nguyen Binh
Photonic Fiber Ring Lasers

MONASH
UNIVERSITY

generation of the laser has been observed and progress of this laser design and experiments will be reported in the near future.
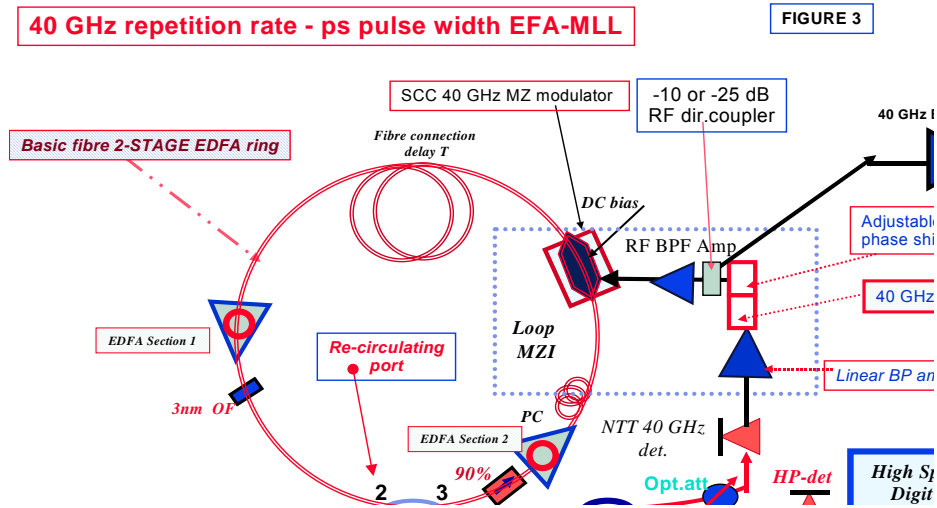
Figure 11 Proposed set up of a 40G regenerative MLRL

2.4   Remarks

We have been successfully constructed a mode locked laser operating under an open loop condition and with O/E RF feedback providing regenerative mode locking. The O/E feedback can certainly provide a self-locking mechanism under the condition that the polarisation characteristics of the ring laser are manageable. This is done by ensuring that all fibers path is under constant operating condition. The regenerative MLRL can self-lock even under the DC drifting effect of the modulator bias voltage (over 20 hours)[3]. The generated pulse trains of 4.5 ps duration can be, without difficulty, compressed further to less than 3 ps for 160 Gb/s optical communication systems.

The regenerative MLRL can be an important source for all-optical switching of an optical packet switching system.

We recommend the following for future works of regenerative MLRL:

- Eliminating polarisation drift through the use of Faraday mirror or all polarisation maintaining (PM) optical components, for example polarised Er-doped fiber amplifiers, PM fiberss at the input and output ports of the intensity modulator;

---

[3] Typically the DC bias voltage of a LiNbO3 intensity modulator is drifted by 1.5 volts after 15 hours of continuous operation.

MONASH
UNIVERSITY

- Stabilising the ring cavity length with appropriate packaging and via piezo/thermal control to improve long term frequency drift;

- Control and automatic tuning of the DC bias voltage of the intensity modulator;

- Developing electronic RF 'clock' recovery circuit for regenerative MLRL operating at 40 GHz repetition rate together with appropriate polarisation control strategy;

- Study of the dependence of the optical power circulating in the ring laser by varying the output average optical power of the optical amplifiers under different pump power conditions;

- Incorporating a phase modulator, in lieu of the intensity modulator, to reduce the complexity of polarisation dependence of the optical waves propagating in the ring cavity, thus minimising the bias drift problem of the intensity modulator.

3   ACTIVE MODE-LOCKED FIBER RING LASER BY RATIONAL HARMONIC DETUNING

In this section we investigate the system behavior of rational harmonic mode-locking in the fiber ring laser using phase plane technique of the nonlinear control engineering. Furthermore, we examine the harmonic distortion contribution to this system performance. We also demonstrate 660x and 1230x repetition rate multiplications on 100MHz pulse train generated from an active harmonically mode-locked fiber ring laser, hence achieve 66GHz and 123GHz pulse operations by using rational harmonic detuning, which is the highest rational harmonic order reported to date.

3.1   Rational harmonic mode-locking

In an active harmonically mode-lock fiber ring laser, the repetition frequency of the generated pulses is determined by the modulation frequency of the modulator, $f_m = qf_c$, where q is the qth harmonic of the fundamental cavity frequency, f_c, which is determined by the cavity length of the laser, $f_c = c/nL$, where c is the speed of light, n is the refractive index of the fiber and L is the cavity length. Typically, f_c is in the range of kHz or MHz. Hence, in order to generate GHz pulse train, mode-locking is normally performed by modulation in the states of $q \gg 1$, i.e. q pulses circulating within the cavity, which is known as harmonic mode-locking. By applying a slight deviation or a fraction of the fundamental cavity frequency, $\Delta f = f_c/m$, where m is the integer, the modulation frequency becomes

$$f_m = qf_c \pm \frac{f_c}{m}$$ (5)

This leads to m-times increase in the system repetition rate, $f_r = mf_m$, where f_r is the repetition

MONASH
UNIVERSITY

frequency of the system [2]. When the modulation frequency is detuned by a m fraction, the contributions of the detuned neighboring modes are weakened, only every m^{th} lasing mode oscillates in phase and the oscillation waveform maximums accumulate, hence achieving in m times higher repetition frequency. However, the small but not negligible detuned neighboring modes affect the resultant pulse train, which leads to uneven pulse amplitude distribution and poor long term stability. This is considered as harmonic distortion in our modeling, and it depends on the laser linewidth and amount of detuned, i.e. fraction m. The amount of the allowable detunes or rather the obtainable increase in the system repetition rate by this technique is very much limited by the amount harmonic distortion. When the amount of frequency detuned is too small relative to the modulation frequency, i.e. large m, contributions of the neighboring lasing modes become prominent, thus reduce the repetition rate multiplication capability significantly. Another words, no repetition frequency multiplication is achieved when the detuned frequency is unnoticeably small. Often the case, it is considered as the system noise due to improper modulation frequency tuning. In addition, the pulse amplitude fluctuation is also determined by this harmonic distortion.

3.2   Experiment setup

The experimental setup of the active harmonically mode-locked fiber ring laser is shown in *Figure 12*. The principal element of the laser is an optical close loop with an optical gain medium, a Mach-Zehnder amplitude modulator (MZM), an optical polarization controller (PC), an optical bandpass filter (BPF), optical couplers and other associated optics.

The gain medium used in our fiber laser system is an erbium doped fiber amplifier (EDFA) with saturation power of 16dBm. A polarization independent optical isolator is used to ensure unidirectional lightwave propagation as well as to eliminate back reflections from the fiber splices and optical connectors. A free space filter with 3dB bandwidth of 4 nm at 1555 nm is inserted into the cavity to select the operating wavelength of the generated signal and to reduce the noise in the system. In addition, it is responsible for the longitudinal modes selection in the mode-locking process. The birefringence of the fiber is compensated by a polarization controller, which is also used for the polarization alignment of the linearly polarized lightwave before entering the planar structure modulator for better output efficiency. Pulse operation is achieved by introducing an asymmetric coplanar traveling wave 10Gb/s lithium niobate, Ti:LiNbO$_3$ Mach-Zehnder amplitude modulator into the cavity with half wave voltage, V$_\pi$ of 5.8 V and insertion loss of $\leq$ 7dB. The modulator is DC biased near the quadrature point and not more than the V$_\pi$ such that it operates around the linear region of its characteristic curve. The modulator is driven by a 100MHz, 100ps step recovery diode (SRD), which is in turn driven by a RF amplifier (RFA) a RF signal generator. The modulating signal generated by the step recovery diode is a ~1% duty cycle Gaussian pulse train. The output coupling of the laser is optimized using a 10/90 coupler. 90% of the optical field power is

MONASH
UNIVERSITY

coupled back into the cavity ring loop, while the remaining portion is taken out as the output of the laser and analyzed.
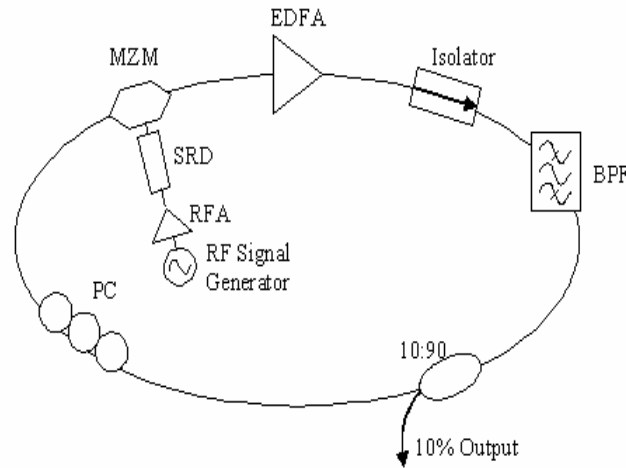
Figure 12: Schematic diagram for active mode-locked fiber ring laser

3.3   Phase plane analysis

Nonlinear system frequently has more than one equilibrium point. It can also oscillate at fixed amplitude and fixed period without external excitation. This oscillation is called limit cycle. However, limit cycles in nonlinear systems are different from linear oscillations. First, the amplitude of self-sustained excitation is independent of the initial condition, while the oscillation of a marginally stable linear system has its amplitude determined by the initial conditions. Second, marginally stable linear systems are very sensitive to changes, while limit cycles are not easily affected by parameter changes [31].

Phase plane analysis is a graphical method of studying second-order nonlinear systems. The result is a family of system motion of trajectories on a two-dimensional plane, which allows us to visually observe the motion patterns of the system. Nonlinear systems can display more complicated patterns in the phase plane, such as multiple equilibrium points and limit cycles. In the phase plane, a limit cycle is defined as an isolated closed curve. The trajectory has to be both closed, indicating the periodic nature of the motion, and isolated, indicating the limiting nature of the cycle [31].

The system modeling of the rational harmonic mode-locked fiber ring laser system is done based on the following assumptions: (i) detuned frequency is perfectly adjusted according to the fraction number required, (ii) small harmonic distortion, (iii) no fiber nonlinearity is included in the analysis, (iv) no other noise sources are involved in the system, and (v) Gaussian

MONASH
UNIVERSITY

lasing mode amplitude distribution analysis.

The phase plane of a perfect 10GHz mode-locked pulse train without any frequency detune is shown *Figure 13* and the corresponding pulse train is shown in *Figure 14*a. The shape of the phase plane exposes the phase between the displacement and its derivative. From the phase plane obtained, one can easily observe that the origin is a stable node and the limit cycle around that vicinity is a stable limit cycle, hence leading to stable system trajectory. 4x multiplication pulse trains, i.e. *m* = 4, without and with 5% harmonic distortion are shown in *Figure 14*b and c. Their corresponding phase planes are shown in *Figure 15*a and b. For the case of zero harmonic distortion, which is the ideal case, the generated pulse train is perfectly multiplied with equal amplitude and the phase plane has stable symmetry periodic trajectories around the origin too. However, for the practical case, i.e. with 5% harmonic distortion, it is obvious that the pulse amplitude is unevenly distributed, which can be easily verified with the experimental results obtained in [3]. Its corresponding phase plane shows more complex asymmetry system trajectories.
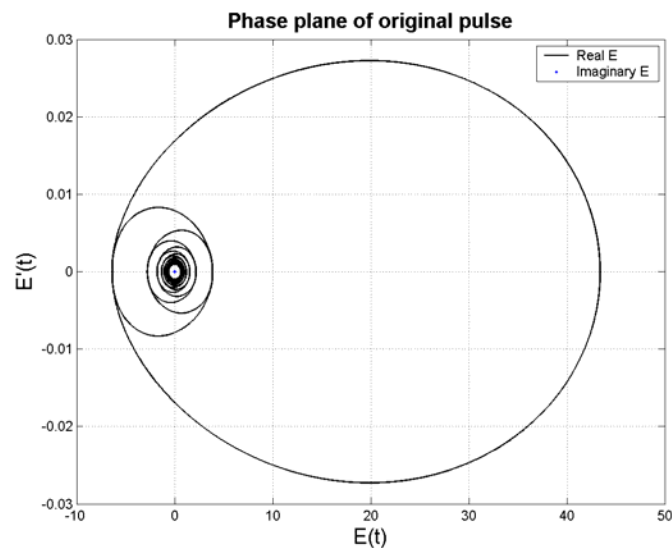
Figure 13: Phase plane of a 10GHz mode-locked pulse train. (solid line – real part of the energy, dotted line – imaginary part of the energy, x-axes – E(t) and y-axes – E'(t))

MONASH
UNIVERSITY
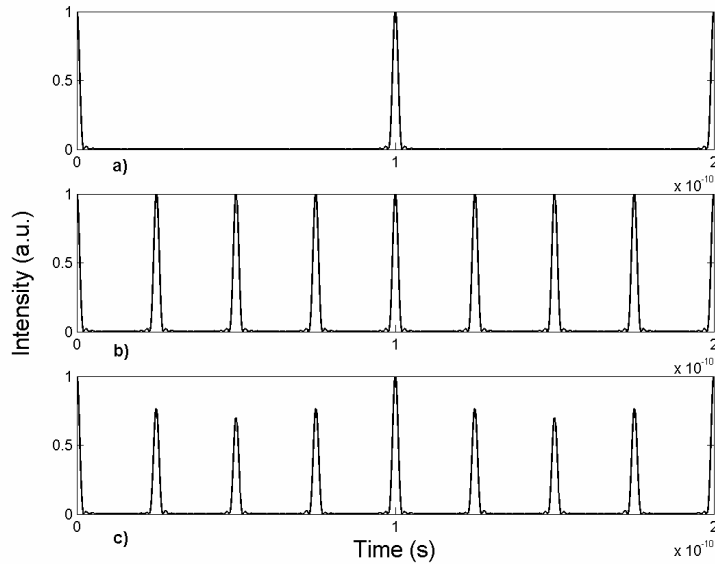
Figure 14: Normalised pulse propagation of original pulse (a); detuning fraction of 4 , with 0% (b) 5% (c) harmonic distortion noise

a)   b)
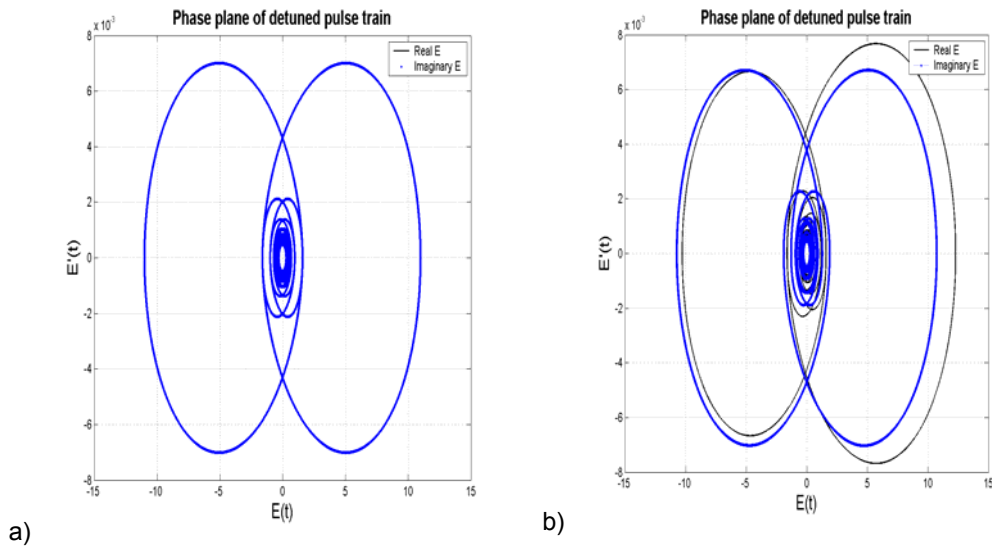
Figure 15: Phase plane of detuned pulse train, m=4, 0% harmonic distortion (a), and 5% harmonic distortion (b) ; (solid line – real part of the energy, dotted line – imaginary part of the energy, x-axes – E(t) and y-axes – E'(t))

One may naively think that the detuning fraction, *m*, could be increased to a very large number, so a very small frequency deviated, *Δf*, so as to obtain a very high repetition frequency. This is only true in the ideal world, if no harmonic distortion is present in the

26

system. However, this is unreasonable for a practical mode-locked laser system.

We define the percentage fluctuation, *%F* as follows:

$$\%F = \frac{E_{max} - E_{min}}{E_{max}} \times 100\%$$ (6)

where E_{max} and E_{min} are the maximum and minimum peak amplitude of the generated pulse train. For any practical mode-locked laser system, fluctuations above 50% should be considered as poor laser system design. Therefore, this is one of the limiting factors in a rational harmonic mode-locking fiber laser system. The relationships between the percentage fluctuation and harmonic distortion for three multipliers (*m*=2, 4 and 8) are shown in the **Figure 15**. Thus, the obtainable rational harmonic mode-locking is very much limited by the harmonic distortion of the system. For 100% fluctuation, it means no repetition rate multiplication, but with additional noise components; a typical pulse train and its corresponding phase plane are shown in *Figure 17* (lower plot) and *Figure 18* with *m*=8 and 20% harmonic distortion. The asymmetric trajectories of the phase graph explain the amplitude unevenness of the pulse train. Furthermore, it shows a more complex pulse formation system. Thus, it is clear that for any harmonic mode-locked laser system, the small side pulses generated are largely due to improper or not exact tuning of the modulation frequency of the system. An experiment result is depicted in *Figure 21* for a comparison.
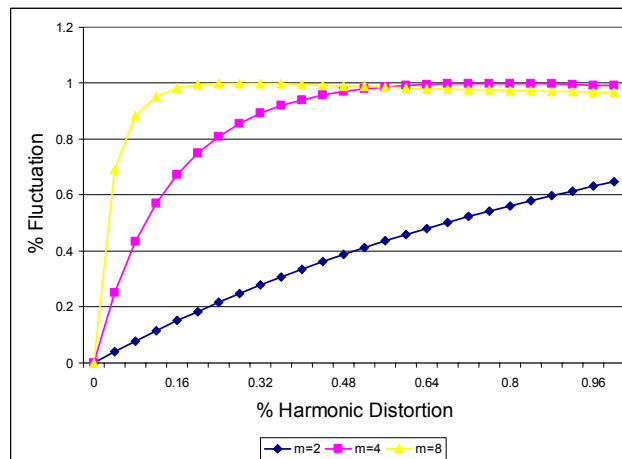
Figure 16: Relationship between the amplitude fluctuation and the percentage harmonic distortion (diamond – m=2, square – m=4, triangle – m=8).

MONASH
U N I V E R S I T Y
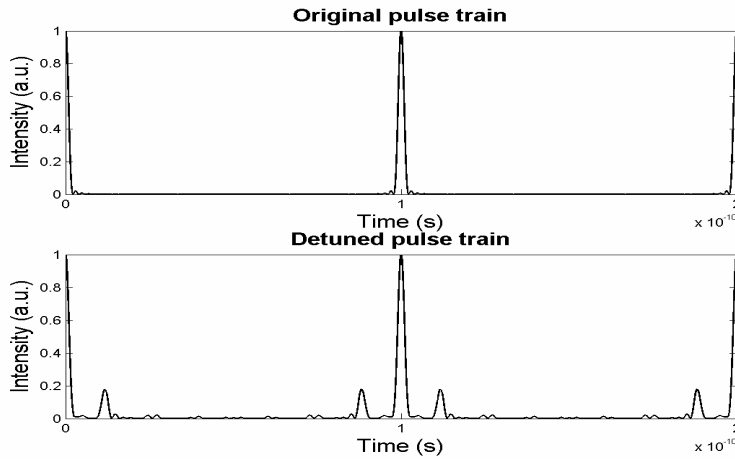
Figure 17: 10GHz pulse train (upper plot), pulse train with m =8 and 20% harmonic distortion (lower plot)
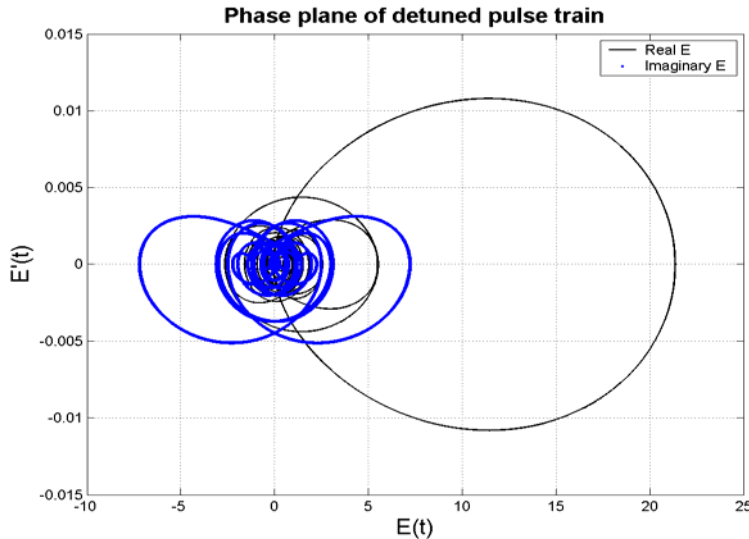
Figure 18: Phase plane of the pulse train with m =8 and 20% harmonic distortion

3.4   Results and discussion

By careful adjustment of the modulation frequency, polarization, gain level and other parameters of the fiber ring laser, we are managed to obtain the 660th and 1230th order of rational harmonic detuning in the mode-locked fiber ring laser with base frequency of 100MHz, hence achieving 66 GHz and 123 GHz repetition frequency pulse operation. The auto-correlation traces and optical spectrums of the pulse operations are shown in *Figure 29*. With Gaussian pulse assumption, the obtained pulse widths of the operations are 2.5456ps and 2.2853ps respectively. For the 100MHz pulse operation, i.e. without any frequency

MONASH
UNIVERSITY

detune, the generated pulse width is about 91ps. Thus, not only we achieved an increase in the pulse repetition frequency, but also a decrease in the generated pulse widths. This pulse narrowing effect is partly due to the self phase modulation effect of the system, as observed in the optical spectrums. Another reason for this pulse shortening is stated by Haus in [18], where the pulse width is inversely proportional to the modulation frequency, as follow:

$$\tau^4 = \frac{2g}{M\omega_m^2 \omega_g^2} \tag{7}$$

where τ is the pulse width of the mode-locked pulse, ω_m is the modulation frequency, g is the gain coefficient, M is the modulation index, and ω_g is the gain bandwidth of the system. In addition, the duty cycle of our Gaussian modulation signal is ~1%, which is very much less than 50%, this leads to a narrow pulse width too. Besides the uneven pulse amplitude distribution, high level of pedestal noise is also observed in the obtained results.

For 66GHz pulse operation, 4nm bandwidth filter is in used in the setup, but it is removed for the 123 GHz operation. It is done so to allow more modes to be locked during the operation, thus, to achieve better pulse quality. In contrast, this increases the level of difficulty significantly in the system tuning and adjustment. As a result, the operation is very much determined by the gain bandwidth of the EDFA used in the laser setup.

a)

b)

c)   d)

© 2005 Le Nguyen Binh
Photonic Fiber Ring Lasers

MONASH
UNIVERSITY
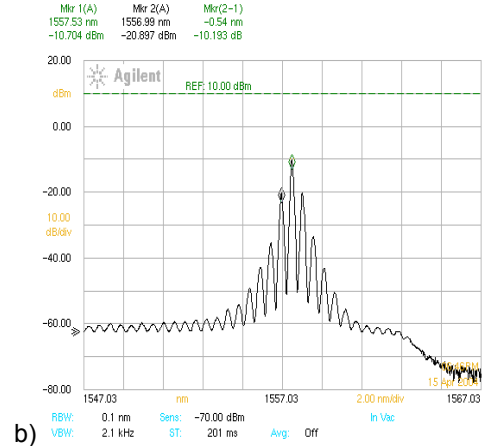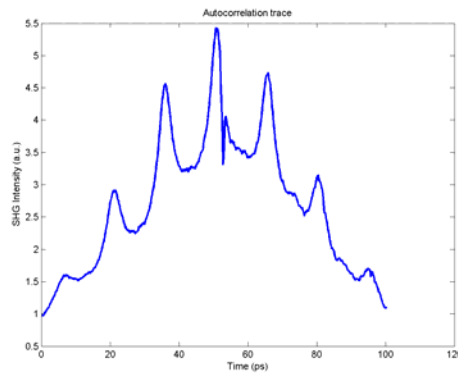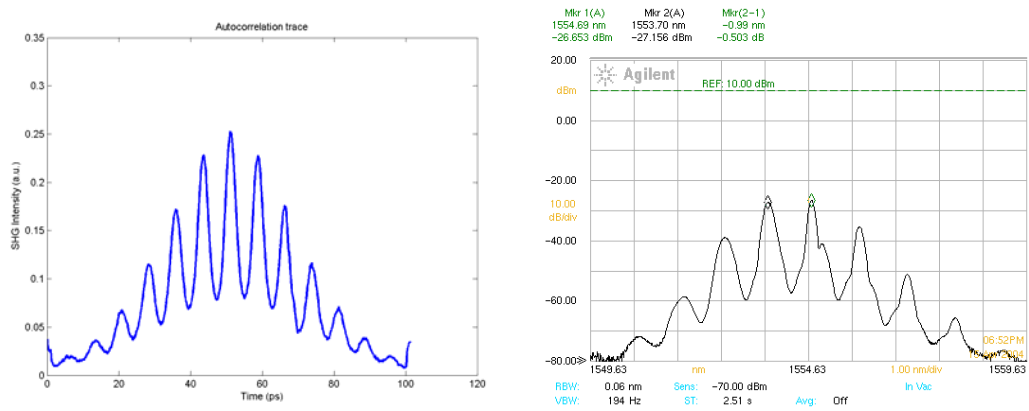
Figure 19: Autocorrelation traces of 66GHz (a) and 123GHz (c) pulse operation; optical spectrums of 66GHz (b) and 123GHz (d)

The simulated phase planes for the above pulse operation are shown in **Figure 20**. They are simulated based on the 100MHz base frequency, 10 round trips condition and 0.001% of harmonic distortion contribution. There is no stable limit cycle in the phase graphs obtained; hence the system stability is hardly achievable, which is a known fact in the rational harmonic mode-locking. Asymmetric system trajectories are observed in the phase planes of the pulse operations. This reflects the unevenness of the amplitude of the pulses generated. Furthermore, more complex pulse formation process is also revealed in the phase graphs obtained.

By a very small amount of frequency deviation, or improper modulation frequency tuning in the general context, we obtain a pulse train with ~100MHz with small side pulses in between as shown in Fig. 10. It is rather similar to the Fig. 6 (lower plot) shown in the earlier section despite the level of pedestal noise in the actual case. This is mainly because we do not consider other sources of noise in our modeling, except the harmonic distortion.

a)   b)

MONASH
UNIVERSITY
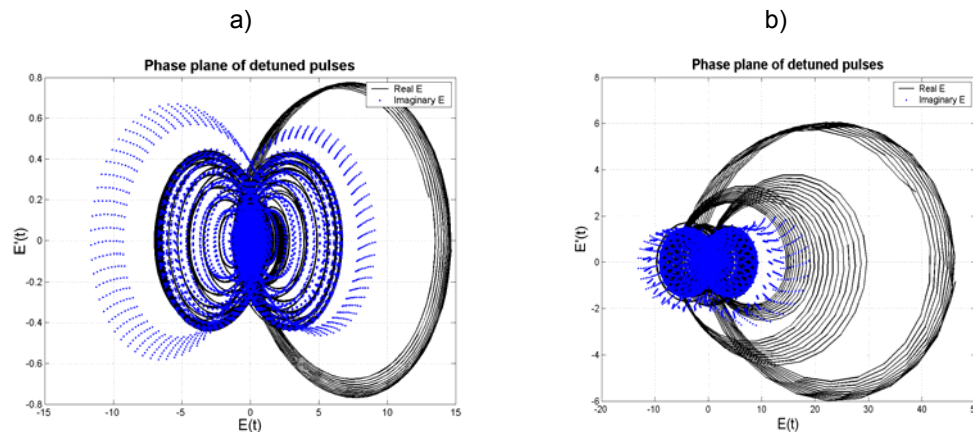
Figure 20: Phase plane of the 66GHz (a) and 123GHz (b) pulse train with 0.001% harmonic distortion noise.

a)
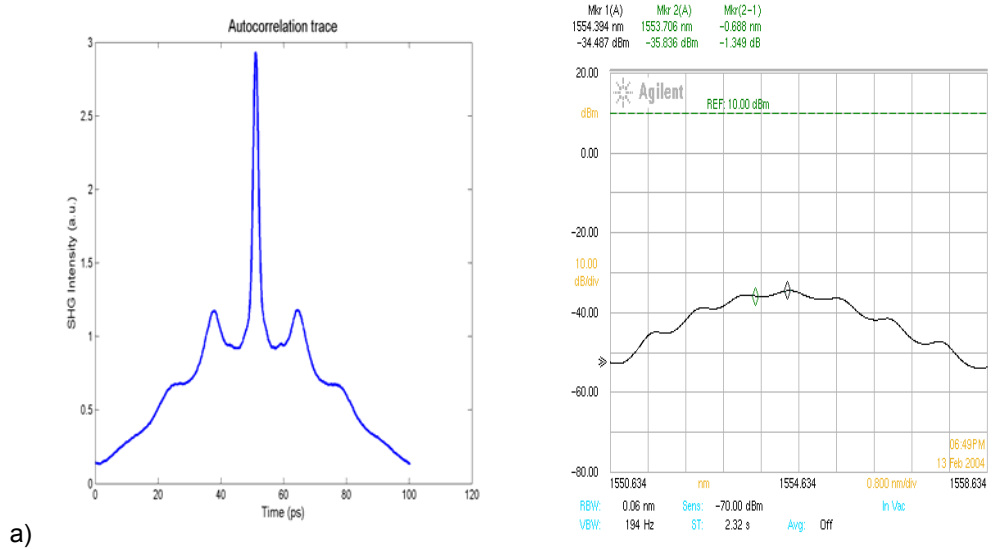
Figure 21: Autocorrelation trace (a) and optical spectrum (b) of slight frequency detune in the mode-locked fiber ring laser

3.5   Concluding remarks

We have demonstrated 660th and 1230th order of rational harmonic mode locking from a base modulation frequency of 100MHz in the erbium doped fiber ring laser, hence achieving 66GHz and 123GHz pulse repetition frequency. To the best of our knowledge, this is the highest rational harmonic order obtained to date. Besides the repetition rate multiplication, we also obtain high pulse compression factor in the system, ~35x and 40x relative to the non-multiplied laser system.

In addition, we use phase plane analysis to study the laser system behavior. From the analysis model, the amplitude stability of the detuned pulse train can only be achieved under negligible or no harmonic distortion condition, which is the ideal situation. The phase plane analysis also reveals the pulse forming complexity of the laser system.

4   REP-RATE MULTIPLICATION RING LASER USING TEMPORAL DIFFRACTION EFFECTS

The pulse repetition rate of a mode-locked ring laser is usually limited by the bandwidth of the intracavity modulator. Hence, a number of techniques have to be used to increase the repetition frequency of the generated pulse train. Rational harmonic detuning [3, 16] is achieved by applying a slight deviated frequency from the multiple of fundamental cavity

MONASH
UNIVERSITY

frequency. 40Ghz repetition frequency has been obtained by [3] using 10GHz base band modulation frequency with 4th order rational harmonic mode locking. This technique is simple in nature. However, this technique suffers from inherent pulse amplitude instability, which includes both amplitude noise and inequality in pulse amplitude, furthermore, it gives poor long-term stability. Hence, pulse amplitude equalization techniques are often applied to achieve better system performance [2], [4, 5]. Fractional temporal Talbot based repetition rate multiplication technique [4-8] uses the interference effect between the dispersed pulses to achieve the repetition rate multiplication. The essential element of this technique is the dispersive medium, such as linearly chirped fiber grating (LCFG) [8, 16] and single mode fiber [8, 9]. This technique will be discussed further in Section II. Intracavity optical filtering [13, 14] uses modulators and a high finesse Fabry-Perot filter (FFP) within the laser cavity to achieve higher repetition rate by filtering out certain lasing modes in the mode-locked laser. Other techniques used in repetition rate multiplication include higher order FM mode-locking [13], optical time domain multiplexing, etc.

The stability of high repetition rate pulse train generated is one of the main concerns for practical multi-Giga bits/sec optical communications system. Qualitatively, a laser pulse source is considered as stable if it is operating at a state where any perturbations or deviations from this operating point is not increased but suppressed. Conventionally the stability analyses of such laser systems are based on the linear behavior of the laser in which we can analytically analyze the system behavior in both time and frequency domains. However, when the mode-locked fiber laser is operating under nonlinear regime, none of these standard approaches can be used, since direct solution of nonlinear different equation is generally impossible, hence frequency domain transformation is not applicable. Although Talbot based repetition rate multiplication systems are based on the linear behavior of the laser, there are still some inherent nonlinearities affecting its stability, such as the saturation of the embedded gain medium, non-quadrature biasing of the modulator, nonlinearities in the fiber, etc., hence, nonlinear stability approach must be adopted.

We investigate the stability and transient analyses of the Group Velocity Dispersion (GVD) multiplied pulse train using the phase plane analysis of nonlinear control analytical technique [2]. ***This is the first time, to the best of our knowledge that the phase plane analysis of modern control engineerin, is being used to study the stability and transient performances of the GVD repetition rate multiplication systems.***

The stability and the transient response of the multiplied pulses are studied using the phase plane technique of nonlinear control engineering. We also demonstrated four times repetition rate multiplication on 10Gbits/s pulse train generated from the active harmonically mode-locked fiber ring laser, hence achieving 40Gbits/s pulse train by using fiber GVD effect. It has been found that the stability of the GVD multiplied pulse train, based on the phase plane analysis is hardly achievable even under the perfect multiplication conditions. Furthermore,

MONASH
UNIVERSITY

uneven pulse amplitude distribution is observed in the multiplied pulse train. In addition to that, the influences of the filter bandwidth in the laser cavity, nonlinear effect and the noise performance are also studied in our analyses.

In Section 4.1, the GVD repetition rate multiplication technique is briefly given. Section 4.2 describes the experimental setup for the repetition rate multiplication. Section 4.4 investigates the dynamic behavior of the phase plane of GVD multiplication system, followed by simulation and experimental results. Finally, some concluding remarks and possible future developments are given.

4.1   GVD Repetition rate multiplication technique

When a pulse train is transmitted through an optical fiber, the phase shift of kth individual lasing mode due to group velocity dispersion (GVD) is

$$\varphi_k = \frac{\pi\lambda^2 D z k^2 f_r^2}{c} \tag{8}$$

where λ is the center wavelength of the mode-locked pulses, D is the fiber's GVD factor, z is the fiber length, f_r is the repetition frequency and c is the speed of light in vacuum. This phase shift induces pulse broadening and distortion. At Talbot distance, $z_T = 2/\Delta\lambda f_r / D /$ [6] the initial pulse shape is restored, where $\Delta\lambda = f_r \lambda^2/c$ is the spacing between Fourier-transformed spectrum of the pulse train. When the fiber length is equal to $z_T/(2m)$, (where m = 2,3,4, …), every m^{th} lasing modes oscillates in phase and the oscillation waveform maximums accumulate. However, when the phases of other modes become mismatched, this weakens their contributions to pulse waveform formation. This leads to the generation of a pulse train with a multiplied repetition frequency with m-times. The pulse duration does not change that much even after the multiplication, because every m^{th} lasing mode dominates in pulse waveform formation of m-times multiplied pulses. The pulse waveform therefore becomes identical to that generated from the mode-locked laser, with the same spectral property. Optical spectrum does not change after the multiplication process, because this technique utilizes only the change of phase relationship between lasing modes and does not use fiber's nonlinearity.

The effect of higher order dispersion might degrade the quality of the multiplied pulses, i.e. pulse broadening, appearance of pulse wings and pulse-to-pulse intensity fluctuation. In this case, any dispersive media to compensate the fiber's higher order dispersion would be required in order to complete the multiplication process. To achieve higher multiplications the input pulses must have a broad spectrum and the fractional Talbot length must be very precise in order to receive high quality pulses. If the average power of the pulse train induces the nonlinear suppression and experience anomalous dispersion along the fiber, solitonic

MONASH
UNIVERSITY

action would occur and prevent the linear Talbot effect from occurring.

The highest repetition rate obtainable is limited by the duration of the individual pulses, as pulses start to overlap when the pulse duration becomes comparable to the pulse train period, i.e. $m_{max} = \Delta T / \Delta t$, where ΔT is the pulse train period and Δt is the pulse duration.

4.2 Experiment setup

GVD repetition rate multiplication is used to achieve 40Gbits/s operation. The input to the GVD multiplier is a 10.217993Gbits/s laser pulse source, obtained from active harmonically mode-locked fiber ring laser, operating at 1550.2nm.

The principle element of the active harmonically mode-locked fiber ring laser is an optical closed loop with an optical gain medium (i.e. Erbium doped fiber with 980nm pump source), an optical 10GHz amplitude modulator, optical bandpass filter, optical fiber couplers and other associated optics. The schematic construction of the active mode-locked fiber ring laser is shown in *Figure 22*. The active mode-locked fiber laser design is based on a fiber ring cavity where the 25 meter EDF with Er^{3+} ion concentration of $4.7x10^{24}$ ions/m^3 is pumped by two diode lasers at 980 nm: SDLO-27-8000-300 and CosetK1116 with maximum forward pump power of 280mW and backward pump power of 120mW. The pump lights are coupled into the cavity by the 980/1550 nm WDM couplers; with insertion loss for 980 nm and 1550 nm signals are about 0.48 dB and 0.35 dB respectively. A polarization independent optical isolator ensures the unidirectional lasing. The birefringence of the fiber is compensated by a polarization controller (PC). A tunable FP filter with 3dB bandwidth of 1 nm and wavelength tuning range from 1530 nm to 1560 nm is inserted into the cavity to select the center wavelength of the generated signal as well as to reduce the noise in the system. In addition, it is used for the longitudinal modes selection in the mode-locking process. Pulse operation is achieved by introducing a JDS Uniphase 10Gb/s lithium niobate, $Ti:LiNbO_3$ Mach-Zehnder amplitude modulator into the cavity with half wave voltage, V_π of 5.8 V. The modulator is DC biased near the quadrature point and not more than the V_π such that it operates on the linear region of its characteristic curve and driven by the sinusoidal signal derived from an Anritsu 68347C Synthesizer Signal Generator. The modulating depth should be less than unity to avoid signal distortion. The modulator has an insertion loss of $\leq$ 7dB. The output coupling of the laser is optimized using a 10/90 coupler. 90% of the optical field power is coupled back into the cavity ring loop, while the remaining portion is taken out as the output of the laser and is analyzed using a New Focus 1014B 40 GHz photo-detector, Ando AQ6317B Optical Spectrum Analyzer, Textronix CSA 8000 80E01 50GHz Communications Signal Analyzer or Agilent E4407B RF Spectrum Analyzer.

MONASH
UNIVERSITY
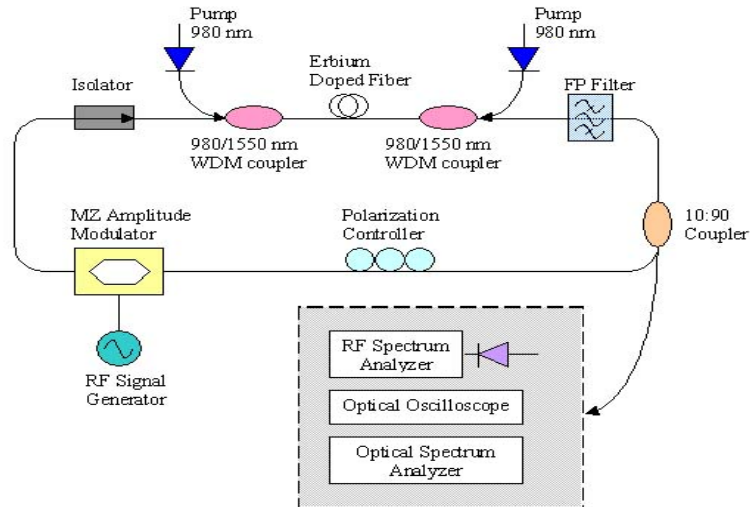
Figure 22: Schematic diagram for active mode-locked fiber ring laser

One rim of about 3.042km of dispersion compensating fiber (DCF), with a dispersion value of -98ps/nm/km was used in the experiment; the schematic of the experimental setup is shown in *Figure 23*. The variable optical attenuator used in the setup is to reduce the optical power of the pulse train generated by the mode-locked fiber ring laser, hence to remove the nonlinear effect of the pulse. An DCF length for 4x multiplication factor on the ~10 GHz signal is required and estimated to be 3.048173 km. The output of the multiplier (i.e. at the end of DCF) is then observed using Textronix CSA 8000 80E01 50GHz Communications Signal Analyzer.
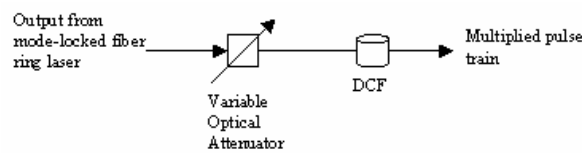
Figure 23: Experiment setup for GVD repetition rate multiplication system

4.3 Phase plane analysis

Nonlinear system frequently has more than one equilibrium point. It can also oscillate at fixed amplitude and fixed period without external excitation. This oscillation is called limit cycle. However, limit cycles in nonlinear systems are different from linear oscillations. First, the amplitude of self-sustained excitation is independent of the initial condition, while the oscillation of a marginally stable linear system has its amplitude determined by the initial conditions. Second, marginally stable linear systems are very sensitive to changes, while limit

MONASH
UNIVERSITY

cycles are not easily affected by parameter changes.

Phase plane analysis is a graphical method of studying second-order nonlinear systems. The result is a family of system motion of trajectories on a two-dimensional plane, which allows us to visually observe the motion patterns of the system. Nonlinear systems can display more complicated patterns in the phase plane, such as multiple equilibrium points and limit cycles. In the phase plane, a limit cycle is defined as an isolated closed curve. The trajectory has to be both closed, indicating the periodic nature of the motion, and isolated, indicating the limiting nature of the cycle.

The system modeling for the GVD multiplier is done based on the following assumptions: (i) perfect output pulse from the mode-locked fiber ring laser without any timing jitter, (ii) the multiplication is achieved under ideal conditions (i.e. exact fiber length for a certain dispersion value), (iii) no fiber nonlinearity is included in the analysis of the multiplied pulse, (iv) no other noise sources are involved in the system, and (v) uniform or Gaussian lasing mode amplitude distribution.

3.4.1   Uniform Lasing Mode Amplitude Distribution

Uniform lasing mode amplitude distribution is assumed at the first instance, i.e. ideal mode-locking condition. The simulation is done based on the 10Gbits/s pulse train, centered at 1550 nm, with fiber dispersion value of –98ps/km/nm, 1 nm flat-top passband filter is used in the cavity of mode-locked fiber laser. The estimated Talbot distance is 25.484km.
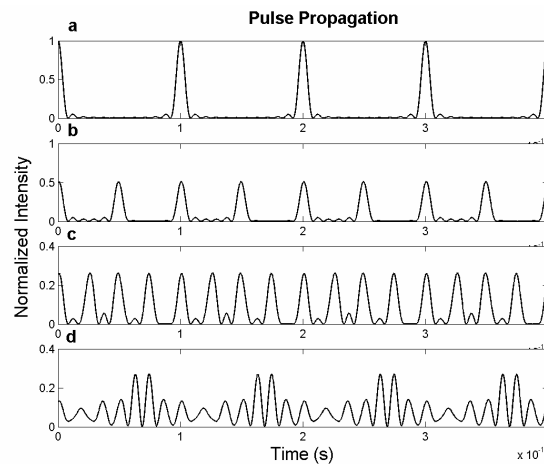

Figure 24: Pulse propagation of (a) original pulse, (b) 2x multiplication , (c) 4x multiplication, and d)8x multiplication with 1nm filter bandwidth and equal lasing mode amplitude analysis

MONASH
UNIVERSITY

Figure 25: Phase plane of (a)original pulse, (b) 2x multiplication , (c) 4x multiplication, and d)8x multiplication with 1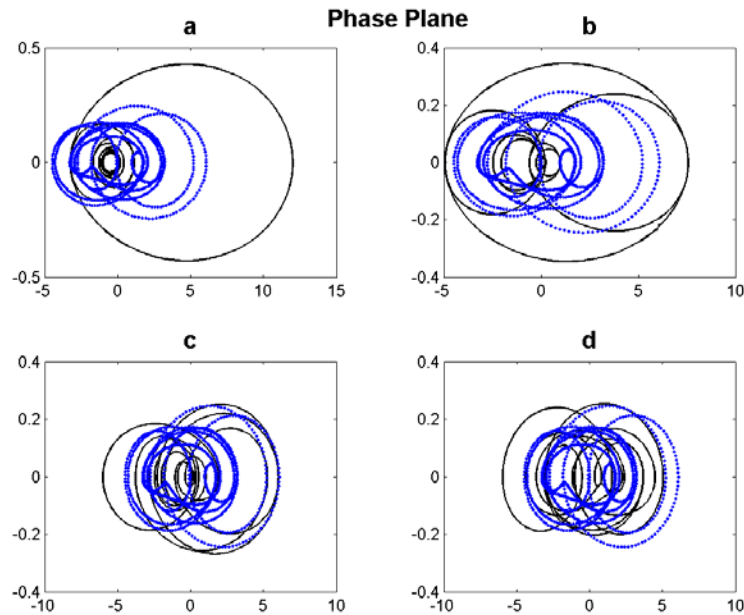nm filter bandwidth and equal lasing mode amplitude analysis; (solid line – real part of the energy, dotted line – imaginary part of the energy, x-axes – E(t) and y-axes – E'(t))

The original pulse (direct from the mode-locked laser) propagation behavior and its phase plane are shown in *Figure 24*a and *Figure 25*a. From the phase plane obtained, one can observe that the origin is a stable node and the limit cycle around that vicinity is a stable limit cycle. This agrees very well to our first assumption: ideal pulse train at the input of the multiplier. Also, we present the pulse propagation behavior and phase plane for 2-times, 4-times and 8-times GVD multiplication system in *Figure 24* and *Figure 25*. The shape of the phase graph exposes the phase between the displacement and its derivative.

As the multiplication factor increases, the system trajectories are moving away from the origin. As for the 4-times and 8-times multiplications, there is neither stable limit cycle nor stable node on the phase planes even with the ideal multiplication parameters. Here we see the system trajectories spiral out to an outer radius and back to inner radius again. The change in the radius of the spiral is the transient response of the system. Hence, with the increase in multiplication factor, the system trajectories become more sophisticated. Although GVD repetition rate multiplication uses only the phase change effect in multiplication process, the inherent nonlinearities still affect its stability indirectly. Despite the reduction in the pulse amplitude, we observe uneven pulse amplitude distribution in the multiplied pulse train. The percentage of unevenness increases with the multiplication factor in the system.

3.4.2   Gaussian Lasing Mode Amplitude Distribution

This set of the simulation models the practical filter used in the system. It gives us a better insight on the GVD repetition rate multiplication system behavior. The parameters used in the simulation are exactly the same except the filter of the laser has been changed to 1 nm (125GHz @ 1550nm) Gaussian-profile passband filter. The spirals of the system trajectories and uneven pulse amplitude distribution are more severe than those in the uniform lasing mode amplitude analysis.

Figure 26: Pulse propagation of (a)original pulse, (b) 2x multiplication , (c) 4x multiplication, , and (d)8x multiplication with 1nm filter bandwidth and Gaussian lasing mode amplitude analysis

MONASH
UNIVERSITY
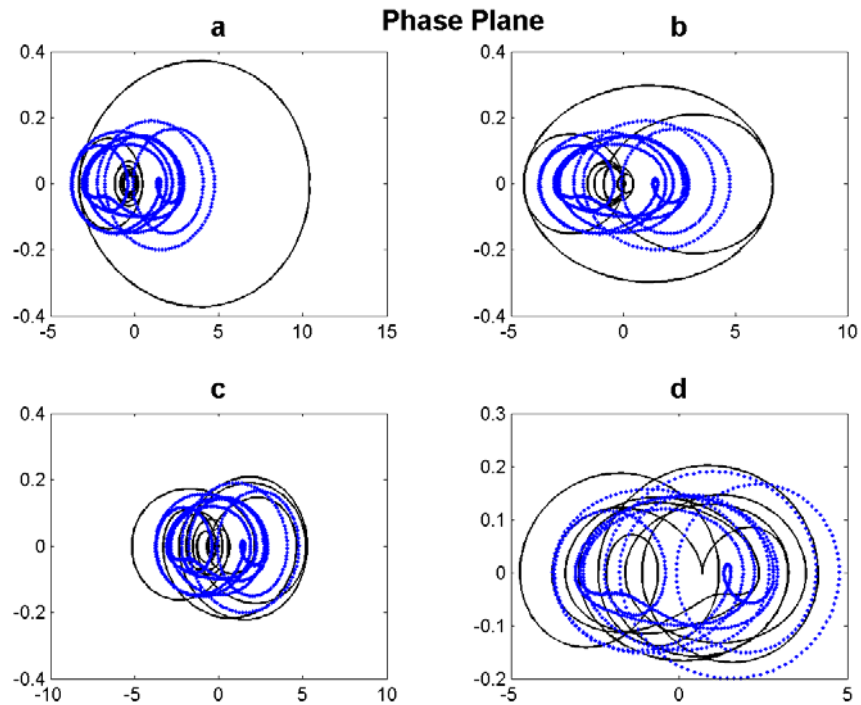
Figure 27: Phase plane of (a) original pulse, (b) 2x multiplication , (c) 4x multiplication, and (d) 8x multiplication with 1nm filter bandwidth and Gaussian lasing mode amplitude analysis; (solid line – real part of the energy, dotted line – imaginary part of the energy, x-axes – E(t) and y-axes – E'(t))

3.4.3   Effects of Filter Bandwidth

Filter bandwidth used in the mode-locked fiber ring laser will affect the system stability of the GVD repetition rate multiplication system as well. The analysis done above is based on 1 nm filter bandwidth. The number of modes locked in the laser system increases with the bandwidth of the filter used, which gives us a better quality of the mode-locked pulse train. The simulation results shown below are based on the Gaussian lasing mode amplitude distribution, 3nm filter bandwidth used in the laser cavity, and other parameters remain unchanged.
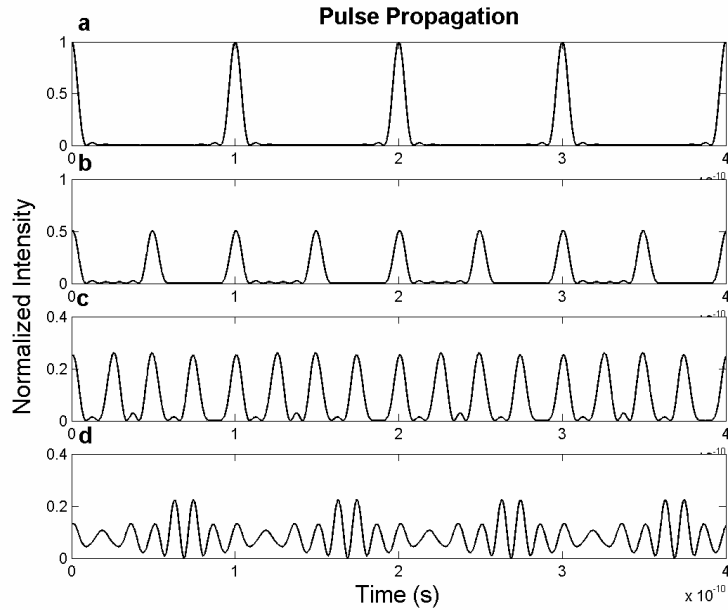
Figure 28: Pulse propagation of (a) original pulse, (b) 2x multiplication , (c) 4x multiplication, and (d) 8x multiplication with 3nm filter bandwidth and Gaussian lasing mode amplitude analysis

Figure 29: Phase plane of (a)original pulse, (b) 2x multiplication , (c) 4x multiplication, and (d) 8x multiplication with 3nm filter bandwidth and gaussian lasing mode amplitude analysis; (solid line – real part of the energy, dotted line – imaginary part of the energy, x-axes – E(t) and y-axes – E'(t))

With wider filter bandwidth, the pulse width and the percentage pulse amplitude fluctuation

MONASH
UNIVERSITY

decreases. This suggests a better stability condition. Instead of spiraling away from the origin, the system trajectories move inward to the stable node. However, this leads to a more complex pulse formation system.

3.4.4   Nonlinear Effects

When the input power of the pulse train enters the nonlinear region, the GVD multiplier loses its multiplication capability as predicted. The additional nonlinear phase shift due to the high input power is added to the total pulse phase shift and destroys the phase change condition of the lasing modes required by the multiplication condition. Furthermore, this additional nonlinear phase shift also changes the pulse shape and the phase plane of the multiplied pulses.
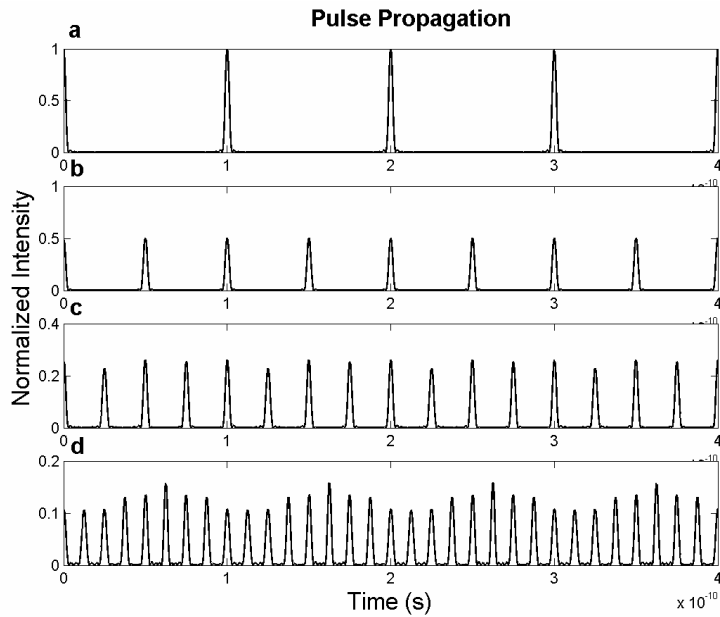

Figure 30: Pulse propagation of (a) original pulse, (b) 2x multiplication , (c) 4x multiplication, and (d)8x multiplication with 3nm filter bandwidth, Gaussian lasing mode amplitude analysis and input power = 1W

MONASH
UNIVERSITY

Figure 31: Phase plane of (a) original pulse,(b) 2x multiplication , (c) 4x multiplication, and (d) 8x multiplication with 3nm filter bandwidth, Gaussian lasing mode amplitude analysis an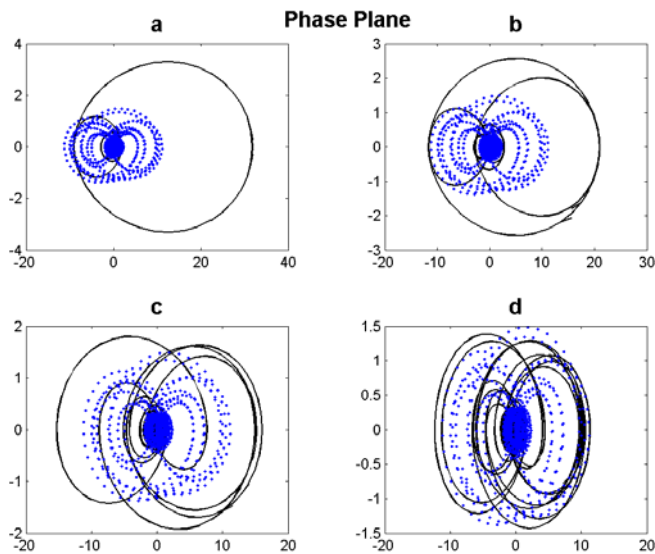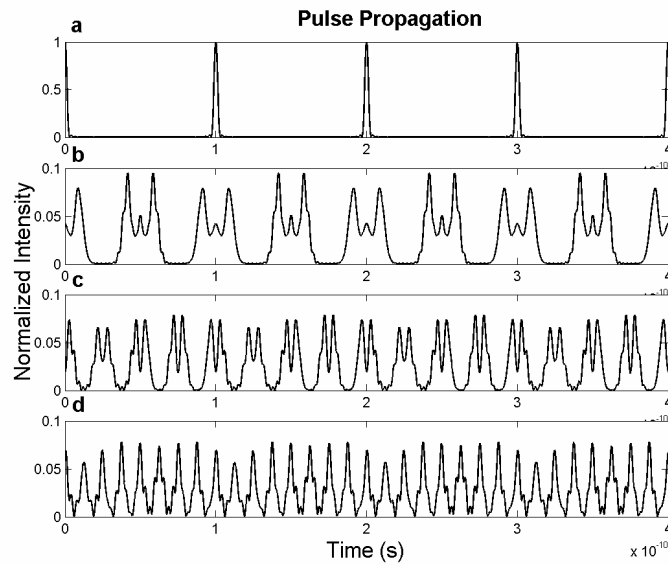d input power = 1W; (solid line – real part of the energy, dotted line – imaginary part of the energy, x-axes – E(t) and y-axes – E'(t))

3.4.5   Noise Effects

The above simulations are all based on the noiseless situation. However, in the practical optical communication systems, noises are always sources of nuisance which can cause system instability, therefore it must be taken into the consideration for the system stability studies.

Since the optical intensity of the m-times multiplied pulse is m-times less than the original pulse, it is more vulnerable to noise. The signal is difficult to differentiate from the noise within the system if the power of multiplied pulse is too small. The phase plane the multiplied pulse is distorted due to the presence of the noise, which leads to poor stability performance.

Figure 32: *Pulse propagation of (a)original pulse, (b)2x multiplication , (c) 4x multiplication, and (d) 8x multiplication with 3nm filter bandwidth, Gaussian lasing mode amplitude analysis and 0dB signal to noise ratio*
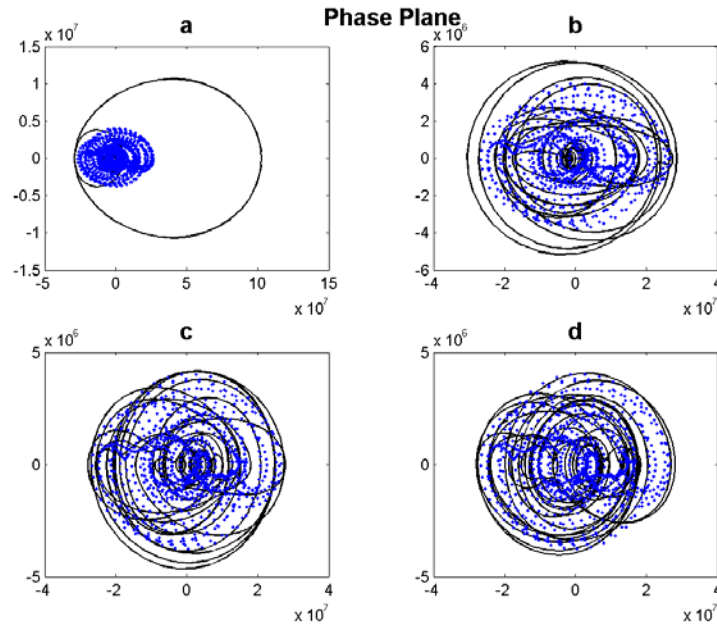

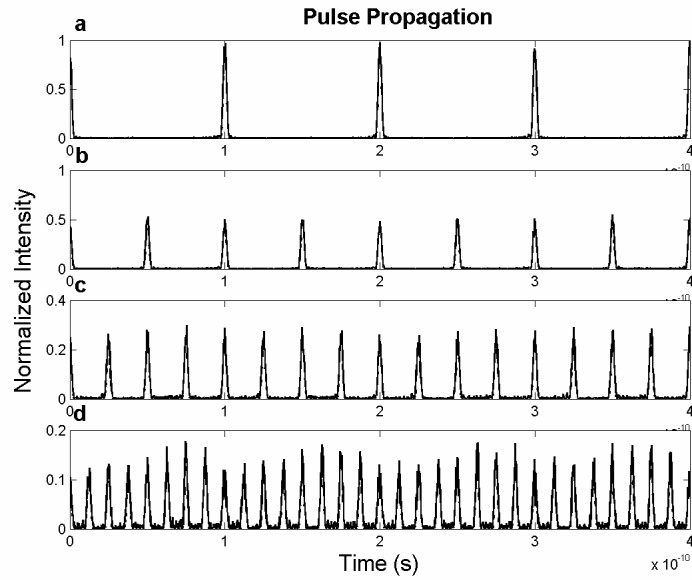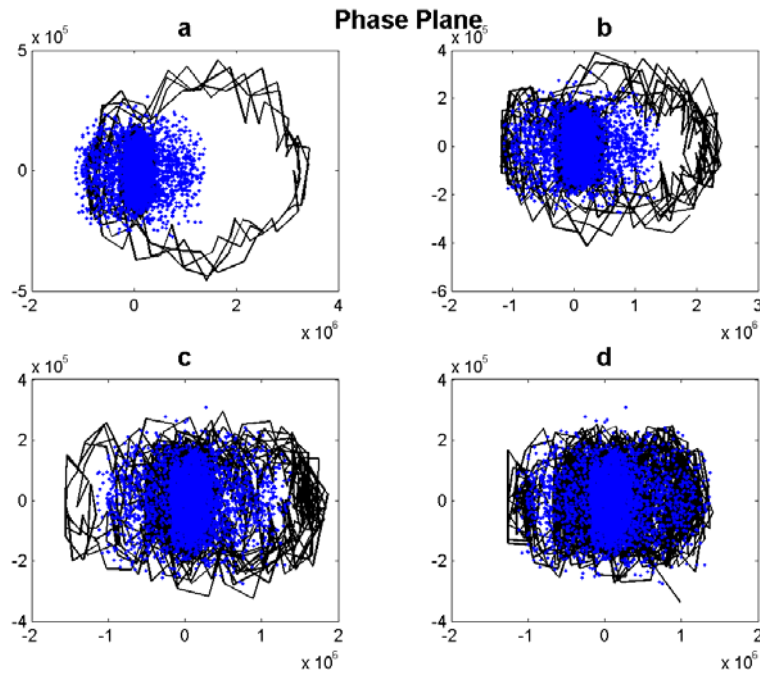*Figure 33:* *Phase plane of (a) original pulse, (b)2x multiplication , (c) 4x multiplication, and (d)8x multiplication with 3nm filter bandwidth, gaussian lasing mode amplitude analysis and 0dB signal to noise ratio; (solid line – real part of the energy, dotted line – imaginary part of the energy, x-axes – E(t) and y-axes – E'(t))*

4.4 Demonstration

The obtained 10 GHz output pulse train from the mode-locked fiber ring laser is shown in *Figure 34*. Its spectrum is shown in *Figure 35*. This output was then used as the input to the dispersion compensating fiber, which acts as the GVD multiplier in our experiment. The obtained 4-times multiplication by the GVD effect and its spectrum are shown in *Figure 37* and *Figure 37*

The spectrums for both cases (original and multiplied pulse) are exactly the same since this repetition rate multiplication technique utilizes only the change of phase relationship between lasing modes and does not use fiber's nonlinearity.

The multiplied pulse suffers an amplitude reduction in the output pulse train; however, the pulse characteristics should remain the same. The instability of the multiplied pulse train is mainly due to the slight deviation from the required DCF length (0.2% deviation). Another reason for the pulse instability, which derived from our analysis; is the divergence of the pulse energy variation in the vicinity around the origin, as the multiplication factor gets higher. The pulse amplitude decreases with the increase in multiplication factor, as the fact of energy conservation, when it reaches certain energy level, which is indistinguishable from the noise level in the system, the whole system will become unstable and noisy.
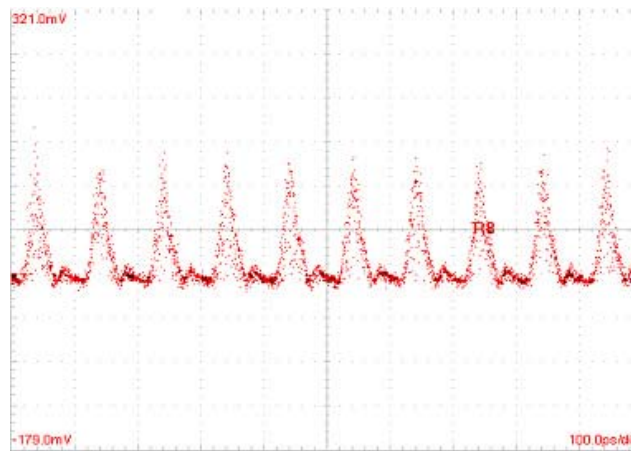
Figure 34: 10 GHz pulse train from mode-locked fiber ring laser (100ps/div, 50mV/div)

MONASH
UNIVERSITY

Figure 35: 10 GHz pulse spectrum from mode-locked fiber ring laser

Figure 36: 40GHz multiplied pulse train (20ps/div, 1mV/div)

Figure 37: 40 GHz pulse spectrum from GVD multiplier

MONASH
U N I V E R S I T Y

4.5   Concluding remarks

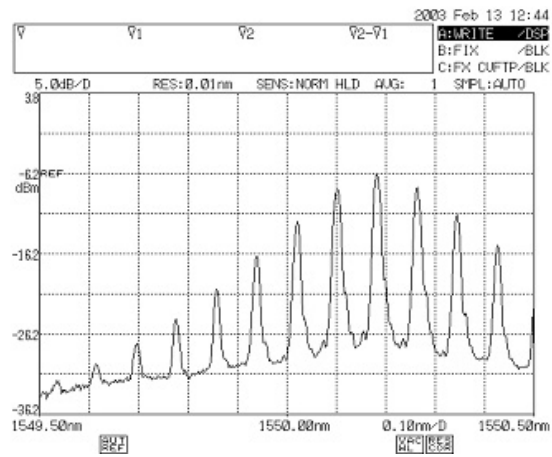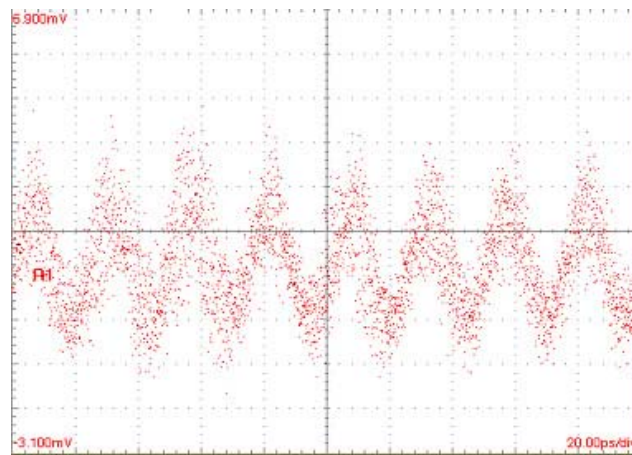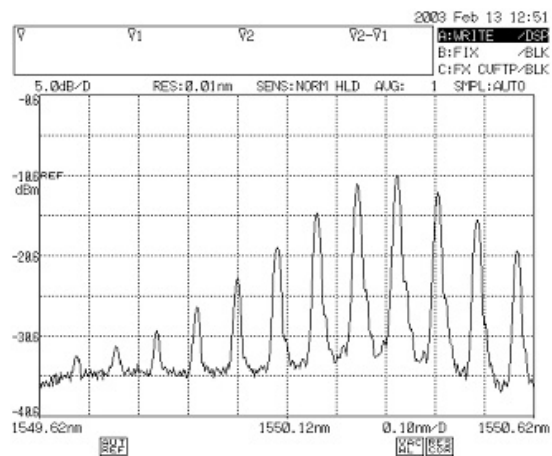We have demonstrated 4-times repetition rate multiplication by using fiber GVD effect; hence, 40GHz pulse train is obtained from 10GHz mode-locked fiber laser source. However, its stability is of great concern for the practical use in the optical communications systems. Although the GVD repetition rate multiplication technique is linear in nature, the inherent nonlinear effects in such system may disturb the stability of the system. Hence any linear approach may not be suitable in deriving the system stability. Stability analysis for this multiplied pulse train has been studied by using the nonlinear control stability theory, which is the first time, to the best of our knowledge, that phase plane analysis is being used to study the transient and stability performance of the GVD repetition rate multiplication system. Surprisingly, from the analysis model, the stability of the multiplied pulse train can hardly be achieved even under perfect multiplication conditions. Furthermore, we observed uneven pulse amplitude distribution in the GVD multiplied pulse train, which is due to the energy variations between the pulses that cause some energy beating between them. Another possibility is the divergence of the pulse energy variation in the vicinity around the equilibrium point that leads to instability.

The pulse amplitude fluctuation increases with the multiplication factor. Also, with wider filter bandwidth used in the laser cavity, better stability condition can be achieved. The nonlinear phase shift and noises in the system challenge the system stability of the multiplied pulses. They not only change the pulse shape of the multiplied pulses, they also distort the phase plane of the system. Hence, the system stability is greatly affected by the self phase modulation as well as the system noises.

This stability analysis model can further be extended to include some system nonlinearities, such as the gain saturation effect, non-quadrature biasing of the modulator, fiber nonlinearities, etc. The chaotic behavior of the system may also be studied by applying different initial phase and injected energy conditions to the model.

5   MULTI-WAVELENGTH FIBER RING LASERS

This section presents the theoretical development and demonstration of a multi-wavelength erbium-doped fiber ring laser with an all-polarization-maintaining fiber (PMF) Sagnac loop. The Sagnac loop simply consists of a PMF coupler and a segment of stress-induced PMF, with a single-polarization coupling point in the loop. The Sagnac loop is shown to be a stable comb filter with equal frequency period which determines the possible output power spectrum of the fiber ring laser. The number of output lasing wavelengths is obtained by adjusting the polarization state of the light in the unidirectional ring cavity by means of a polarization controller. This section is organised as follows: Section 5.1 presents the theory of the Sagnac PMF loop filter, which consists of a PMF coupler (instead of a standard single-mode fiber

MONASH
U N I V E R S I T Y

coupler used in previous works as described above) and a segment of PMF. Section 5.2 presents the experimental results and discussion. Concluding remarks are given in Section 5.3.

5.1 Theory

(a)   (b)
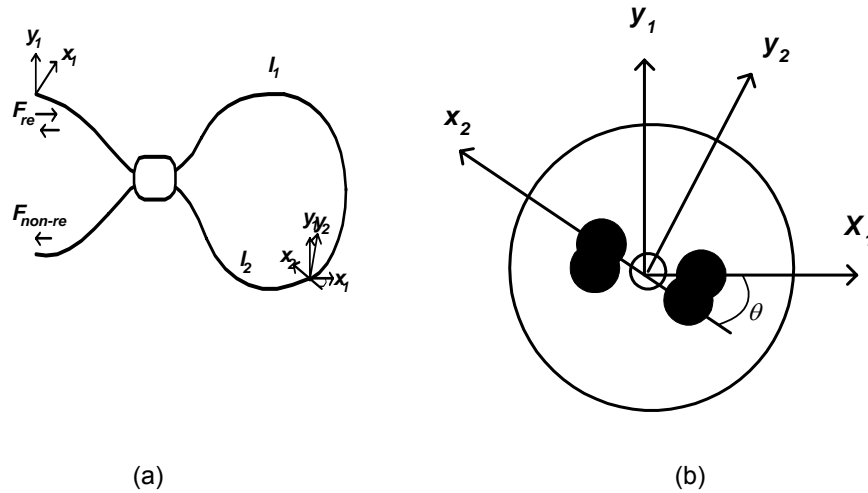
Figure 38 1 (a) Schematic diagram of the proposed all-PMF Sagnac loop filter with a single coupling point. (b) Representation of the coordinates of the single coupling point.

In this section, we present a theoretical analysis of the all-PMF Sagnac loop, which is the key component in the fiber ring laser. We consider the simplest case (see *Figure 38*(a)), in which only one polarization mode-coupling point exists. That is, the loop filter is constructed by splicing the two pigtails (with lengths l_1 and l_2) of the PMF coupler with a phase difference θ along a certain principal axis at the spliced point. The input light is equally split into two waves by the 3-dB PMF coupler, and the two counter-propagating waves are recombined at the coupler output port after traveling through the loop. The electric components, $E_{ix}(\omega)$ and $E_{iy}(\omega)$, of the input light, $E_{in}(\omega)$, can be defined as

$$E_{in}(\omega) = \begin{pmatrix} E_{ix}(\omega) \\ E_{iy}(\omega) \end{pmatrix}$$

(9)

where ω is the angular optical frequency. The PMF with length l can be considered as an ideal waveguide with linear birefringence, which is described by the Jones propagation matrix as [16]

$$J_{PMF}(\omega,l) = \begin{pmatrix} \exp(j\Delta\beta(\omega)l/2) & 0 \\ 0 & \exp(-j\Delta\beta(\omega)l/2) \end{pmatrix} \qquad (10)$$

where $j = \sqrt{-1}$ and $\Delta\beta(\omega) = \beta_x(\omega) - \beta_y(\omega)$ is the difference between the two propagation constants of a high-birefringence fiber which supports two linearly orthogonal fundamental modes (i.e. HE^x_{11} and HE^y_{11}). It should be noted that a common average phase shift of $\exp(j\overline{\beta(\omega)}l)$ is omitted in Eq. (11), because the Sagnac interferometer can not distinguish the common phase term for the clockwise wave (CW) and counter-clockwise wave (CCW). The transfer matrix of the coordinate (i.e. $\Theta(\theta)$) of the polarization mode-coupling point at the principal axes with a phase difference of θ (see *Figure 38*(b)) is given as

$$\Theta(\theta) = \begin{pmatrix} \cos\theta & \sin\theta \\ \sin\theta & -\cos\theta \end{pmatrix} \qquad (11)$$

The 3-dB PMF coupler is assumed to be ideal so that polarization coupling, polarization-dependent loss and frequency dependence of the coupler are negligible (i.e. the coupling ratio is 50% in the operating wavelength range). The CW and CCW will experience the same phase shift and a 3-dB loss through the coupler, thus there is no phase difference at the reciprocal port. Hence, the CW's Jones matrix for the Sagnac loop is given by

$$G_{cw}(\omega) = \frac{1}{2} J_{PMF}(\omega,l_1)\Theta(\theta)J_{PMF}(\omega,l_2) \qquad (12)$$

where $J_{PMF}(\omega,l_1)$ and $J_{PMF}(\omega,l_2)$ are defined in Eq. (12). The CCW's Jones matrix is simply the transpose of the CW's Jones matrix and is given by

$$G_{ccw}(\omega) = G_{cw}^T(\omega) \qquad (13)$$

The electric components of the light at the output ports are given by

$$E_{out}(\omega) = \begin{pmatrix} E_{ox}(\omega) \\ E_{oy}(\omega) \end{pmatrix} \qquad (14)$$

The relationship between the electric components at the input and output ports is given by

$$E_{out}(\omega) = [G_{ccw}(\omega) + G_{cw}(\omega)]E_{in}(\omega) \qquad (15)$$

MONASH
UNIVERSITY

Using Eqs. (1)–(6), the intensity transfer function, F_{re}, for the reciprocal port can be derived as

$$F_{re} = 1 - \sin^2 \theta \cdot \sin^2 \left(\Delta \beta \cdot \Delta l / 2 \right) \tag{16}$$

where $\Delta l = l_2 - l_1$ is the difference between the length of the two PMF segments in the loop. It is noted that Eq. (17) is independent of the polarization state of the input light due to the fact that the interference terms of the *x*-component and *y*-component of the light cancel out with each other at the output port. From Eq. (17), it can be shown that when $\theta \neq 0$ or $\theta \neq \pi$ the spectral peaks of the reflection spectrum will have maximum intensity at frequencies according to

$$\Delta \beta(\omega_m) \cdot \Delta l = 2\pi m \qquad \left(m = 1, 2, \cdots \right) \tag{17}$$

Note that light with frequency ω_m will disappear at the non-reciprocal port for the case of $\theta = \pi/2$ because the transfer function of the non-reciprocal port is $F_{non-re} = 1 - F_{re}$. There are two kinds of high-birefringence fibers, namely, stress-induced birefringent fiber and geometry-induced birefringent fiber, where the former one has greater birefringence. Here we only consider the stress-induced birefringent fiber, where the effective index of each polarization is influenced by stress alone. Thus, the modal birefringence *B* is independent of wavelength over a particular wavelength range, and is given by

$$\Delta \beta(\omega_m) = \frac{2\pi}{\lambda} B \qquad \left(m = 1, 2 \cdots \right) \tag{18}$$

Using Eqs. (18) and (19), the spectral peaks of the reflection spectrum will have maximum intensity at frequencies f_m given by

$$f_m = \frac{mc}{B\Delta l} \qquad \left(m = 1, 2 \cdots \right) \tag{19}$$

where c is the speed of the light in vacuum. From Eq. (20), the Sagnac loop is a comb filter whose spectral peaks are separated by frequency spacing given by

$$f_{m+1} - f_m = \frac{c}{B\Delta l} \tag{20}$$

MONASH
UNIVERSITY

It is noted that although the frequency-dependent intensity transfer function of the loop filter (see Eq. (8)) is independent of the state of polarization of the input light, the polarization state of the output light generally depends on the polarization state and frequency of the input light.
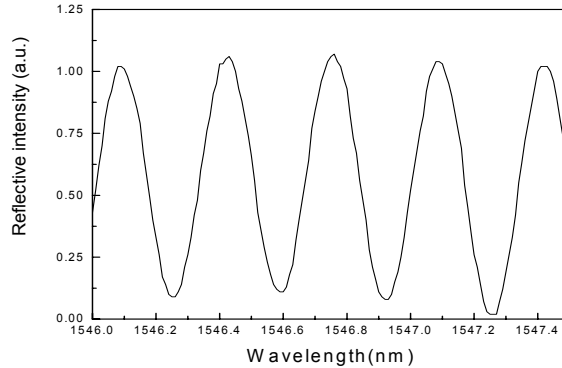
Figure 39 A typical reflective spectrum of the all-PMF Sagnac loop filter with a single coupling point.

5.2 Experimental Results and Discussion

This section presents the experimental verification of the theoretical analysis of the all-PM Sagnac loop filter described in Section 5.1 and the experimental results of the fiber ring laser. *Figure 41* shows a typical reflective spectrum of the all-PMF Sagnac loop filter. The loop filter was constructed by splicing the two pigtails (with lengths l_1 and l_2) of the PMF coupler in 0° and 90° with respect to their principal axes to form a single coupling point in the loop (i.e. a phase difference of $\theta = 90^\circ$). The loop filter is highly stable as expected because all the components used are all-PM components. From *Figure 39*, the frequency period of the filter is 0.35 nm, which agrees well with the theoretical value as predicted by Eq. (21) when the following parameter values, $B = 5.2 \times 10^{-4}$ and $\Delta l = 13.2\,\mathrm{m}$ (in the 1550-nm window) are substituted into the equation.
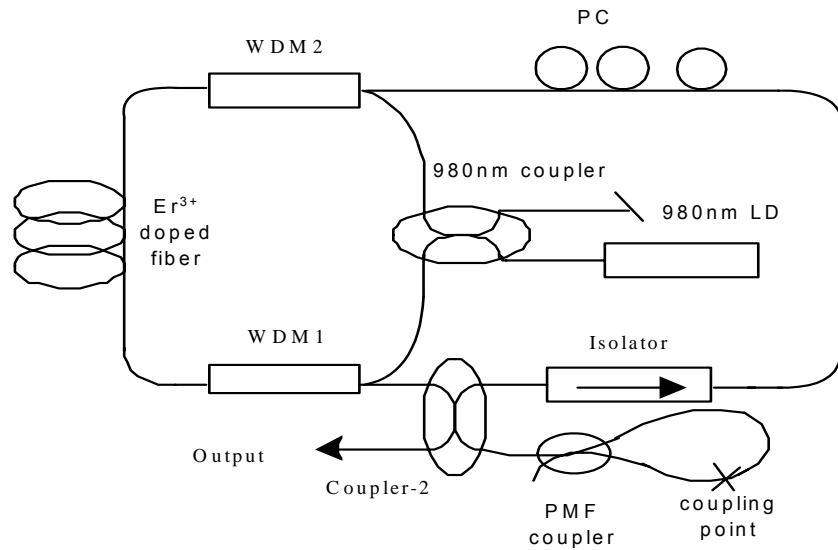
MONASH
UNIVERSITY

Figure 40 *Schematic of the proposed unidirectional fiber ring laser using the all-PMF Sagnac loop as a stable periodic filter.*

Figure 40 shows the schematic diagram of the proposed unidirectional fiber ring laser with the all-PMF Sagnac loop filter. It consists of a 15 m long of Er^{3+} silica fiber doped with ~200 ppm of erbium. The erbium-doped fiber has a numerical aperture (NA) of 0.21, a cut-off wavelength of 920 nm, and an absorption coefficient of 12 dB/m at 980 nm. To increase the optical pump efficiency, the erbium-doped fiber is pumped by a 980-nm laser diode (LD), which generates 70 mW power in both directions in the ring cavity through the two 980/1550-nm WDM couplers. A polarization-independent fiber isolator is used to provide unidirectional ring oscillation so as to avoid spatial hole burning in the gain medium. The coupler-2 is used as the output coupler for the fiber laser and also to direct the light wave to the Sagnac loop filter. The periodic spectral peaks of the Sagnac filter will determine the lasing wavelengths. A polarization controller (PC) is used in the cavity to adjust the polarization state to obtain several lasing wavelengths at the output port.

Figure 41(a) and (b) show the experimental results of the output lasing wavelengths of the fiber ring laser under different polarization conditions by adjusting the PC in the cavity. It can be seen that the wavelength spacing is 1.0 nm, which is defined by the 1.0 nm frequency period of the Sagnac loop filter with parameter values of $B = 5.2 \times 10^{-4}$ and $\Delta l = 4.5 \, \text{m}$. Figure 5 shows the output spectra of the lasing wavelengths of the fiber ring laser under a particular polarization condition in the cavity, where the wavelength spacing is 0.50 nm which is defined by the 0.50 nm frequency period of the Sagnac loop filter with parameter values of $B = 5.2 \times 10^{-4}$ and $\Delta l = 9.0 \, \text{m}$. It should be noted that the number of output lasing wavelengths of the proposed fiber ring laser could be greatly increased by overcoming the large homogeneous broadening of the gain medium of the erbium-doped fiber at room

MONASH
UNIVERSITY

temperature [32]. This problem can be overcome by cooling the erbium-doped fiber to 77 K, but this technique is probably not suitable for practical applications [33]. A more practical approach is to use an acousto-optic frequency shifter in the ring cavity to prevent the steady-state laser oscillation in order to generate a larger number of stable lasing wavelengths [34].

(a)   (b)
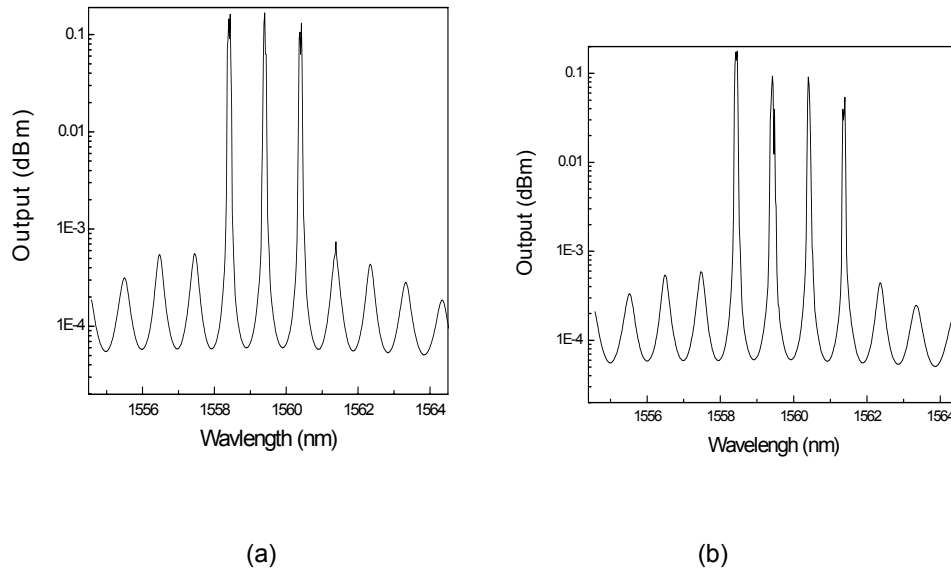
Figure 41 (a), (b) Typical output lasing wavelengths of the fiber ring laser under different polarization conditions of the PC in the ring cavity. Wavelength spacing is 1.0 nm.
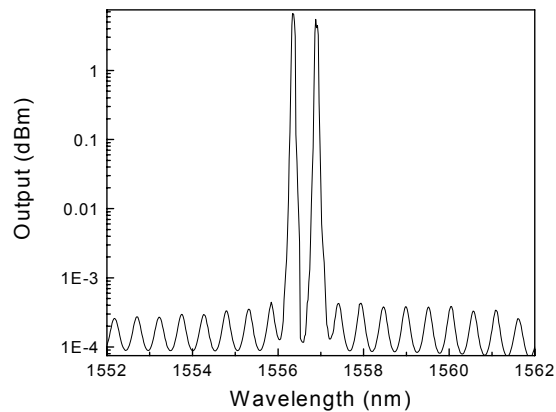

Figure 42 Typical output lasing wavelength of the fiber ring laser under a particular polarization condition of the PC in the ring cavity. Wavelength spacing is 0.50 nm.

MONASH
U N I V E R S I T Y

5.3   Remarks

In this section we have demonstrated an Er:doped fiber ring laser using an all-polarization-maintaining-fiber (PMF) Sagnac loop filter for multi-wavelength operation. The theoretical analysis and experimental results of the all-PMF Sagnac loop as a stable comb filter have been presented. The Sagnac loop filter is a simple and all-fiber device that consists of a PMF coupler and a segment of stress-induced PMF to form the loop. The number of output lasing wavelengths has been obtained by adjusting the polarization state of the light in the ring cavity using a polarization controller. The wavelength spacing is determined by the frequency period of the comb filter with equal frequency interval.

6   CONCLUSIONS

We have been successfully demonstrated a mode locked laser operating under the open loop condition and with O/E RF feedback providing regenerative mode locking. The O/E feedback can certainly provide a self-locking mechanism under the condition that the polarisation characteristics of the ring laser are manageable. The regenerative MLRL can self-lock even under the DC drifting effect of the modulator bias voltage (over 20 hours)[4]. The generated pulse trains of 4.5 ps duration can be, with minimum difficulty, compressed further to less than 3 ps for 160 Gb/s optical communication systems.

We have also demonstrated 660th and 1230th order of rational harmonic mode locking from a base modulation frequency of 100MHz in the optically amplified fiber ring laser, hence achieving 66GHz and 123GHz pulse repetition frequency. ***To the best of our knowledge, this is the highest rational harmonic order obtained to date***. Besides the repetition rate multiplication, we also obtain high pulse compression factor in the system, ~35x and 40x relative to the non-multiplied laser system. In addition, we use phase plane analysis to study the laser system behavior. From the analysis model, the amplitude stability of the detuned pulse train can only be achieved under negligible or no harmonic distortion condition, which is the ideal situation. The phase plane analysis also reveals the pulse forming complexity of the laser system.

We have demonstrated 4-times repetition rate multiplication by using fiber GVD effect; hence, 40GHz pulse train is obtained from 10GHz mode-locked fiber laser source. Stability analysis for this multiplied pulse train has been studied by using the nonlinear control stability theory, which is ***the first time, to the best of our knowledge***, that phase plane analysis is being used to study the transient and stability performance of the GVD repetition rate multiplication system. Surprisingly, from the analysis model, the stability of the multiplied pulse train can hardly be achieved even under perfect multiplication conditions. Furthermore, we observed

---

[4] Typically the DC bias voltage of a LiNbO3 intensity modulator is drifted by 1.5 volts after 15 hours of continuous operation.

© 2005 Le Nguyen Binh
Photonic Fiber Ring Lasers

MONASH
UNIVERSITY

uneven pulse amplitude distribution in the GVD multiplied pulse train, which is due to the energy variations between the pulses that cause some energy beating between them. Another possibility is the divergence of the pulse energy variation in the vicinity around the equilibrium point that leads to instability.

The pulse amplitude fluctuation increases with the multiplication factor. Also, with wider filter bandwidth used in the laser cavity, better stability condition can be achieved. The nonlinear phase shift and noises in the system challenge the system stability of the multiplied pulses. They not only change the pulse shape of the multiplied pulses, they also distort the phase plane of the system. Hence, the system stability is greatly affected by the self phase modulation as well as the system noises. This stability analysis model can further be extended to include some system nonlinearities, such as the gain saturation effect, non-quadrature biasing of the modulator, fiber nonlinearities, etc. The chaotic behavior of the system may also be studied by applying different initial phase and injected energy conditions to the model.

In Section 5 we have demonstrated an erbium-doped fiber ring laser using an all-polarization-maintaining-fiber (PMF) Sagnac loop filter for multi-wavelength operation. The theoretical analysis and experimental results of the all-PMF Sagnac loop as a stable comb filter have been presented. The Sagnac loop filter is a simple and all-fiber device that consists of a PMF coupler and a segment of stress-induced PMF to form the loop. The number of output lasing wavelengths has been obtained by adjusting the polarization state of the light in the ring cavity using a polarization controller. The wavelength spacing is determined by the frequency period of the comb filter with equal frequency interval.

We are currently pursuing the design and demonstration of multi-wavelength mode-locked lasers to generate ultra-short and ultra-high rep-rate pulse sequences by employing a multi-spectral filter demuxes and muxes within the photonic fiber ring. These lasers will be reported in the near future.

© 2005 Le Nguyen Binh
Photonic Fiber Ring Lasers

MONASH
U N I V E R S I T Y

REFERENCES

[1]   K. Kuroda, and H. Takakura, "Mode-locked ring laser with output pulse width of 0.4 ps," *IEEE Trans. Inst. Meas.*, vol. 48, pp. 1018-1022., 1999.

[2]   G. Zhu, H. Chen, and N. Dutta, "Time Domain Analysis of A Rational Harmonic Mode-locked Ring Fiber Laser," *Journal of Applied Physics*, vol. 90, pp. 2143-2147, 2001.

[3]   C. Wu, and N.K. Dutta, "High repetition rate optical pulse generation using a rational harmonic mode-locked fiber laser," *IEEE Journal of Quantum Electronics*, vol. 36, pp. 145-150, 2000.

[4]   K. K. Gupta, N. Onodera and M. Hyodo, "Technique to generate equal amplitude, higher-order optical pulses in rational harmonically modelocked fiber ring lasers," *Electronics Letters*, vol. 37, pp. 948-950, 2001.

[5]   Y. Shiquan, L. Zhaohui, Z. Chunliu, D. Xiaoyi, Y. Shuzhong, K. Guiyun and Z. Qida, "Pulse-Amplitude Equalization in a Raional Harmonic Mode-Locked Fiber Ring Laser by Using Modulator as Both Mode Locker and Equalizer," *IEEE Photonics Technology Letters*, vol. 15, pp. 389-391, 2003.

[6]   J. Azana, and M.A. Muriel, "Technique for Multiplying the Repetition Rates of Periodic Trains of Pulses by Means of a Temporal Self-Imaging Effect in Chirped Fiber Gratings," *Optics Letters*, vol. 24, pp. 1672-1674, 1999.

[7]   S. Atkins, and B. Fischer, "All optical pulse rate multiplication using fractional Talbot effect and field-to-intensity conversion with cross gain modulation," *IEEE Photonics Technology Letters*, vol. 15, pp. 132-134, 2003.

[8]   J. Azana, and M.A. Muriel, "Temporal Self-Imaging Effects: Theory and Application for Multiplying Pulse Repetition Rates," *IEEE Journal of Quantum Electronics*, vol. 7, pp. 728-744, 2001.

[9]   D. A. Chestnut, C. J. S. de Matos and J. R. Taylor, "4x Repetition Rate Multiplication and Raman Compression of Pulses in the Same Optical Fiber," *Optics Letters*, vol. 27, pp. 1262-1264, 2002.

[10]   S. Arahira, S. Kutsuzawa, Y. Matsui, D. Kunimatsu, and Y. Ogawa, "Repetition Frequency Multiplication of Mode-locked Using Fiber Dispersion," *Journal of Lightwave Technology*, vol. 16, pp. 405-410, 1998.

[11]   W. J. Lai, P. Shum, and L.N. Binh, "Stability and Transient Analyses of Temporal Talbot-Effect-Based Repetition-Rate Multiplication Mode-Locked Laser Systems," *IEEE Photonics Technology Letters*, vol. 16, pp. 437-439, 2004.

[12]   K. K. Gupta, N. Onodera, K.S. Abedin and M. Hyodo,, "Pulse Repetition Frequency Multiplication via Intracavity Optical Filtering in AM Mode-locked Fiber Ring Lasers," *IEEE Photonics Technology Letters*, vol. 14, pp. 284-286, 2002.

[13]   K. S. Abedin, N. Onodera and M. Hyodo, "Repetition-rate Multiplication in Actively Mode-locked Fiber Lasers by Higher-order FM Mode-locking Using a High Finesse Fabry Perot Filter," *Applied Physics Letters*, vol. 73, pp. 1311-1313, 1998.

[14]   K. S. Abedin, N. Onodera and M. Hyodo, "Higher Order FM Mode-locking for Pulse-Repetition-Rate Enhancement in Actively Mode-locked Lasers: Theory and Experiment," *IEEE Journal of Quantum Electronics*, vol. 35, pp. 875-890, 1999.

[15]   W. Daoping, Z. Yucheng, L. Tangjun and J. Shuisheng, "20 Gb/s Optical Time Division Multiplexing Signal Generation by Fiber Coupler Loop-Connecting Configuration," presented at 4th Optoelctronics and Communications Conference,, 1999.

[16]   D. L. A. Seixasn, and M.C.R. Carvalho, "50 GHz Fiber Ring Laser Using Rational Harmonic Mode-locking," presented at Microwave and Optoelectronics Conference, 2001.

[17]   R. Y. Kim, "Fiber lasers and their applications," presented at Laser and Electro-Optics, CLEO/Pacific Rim'95,, 1995.

[18]   H. Zmuda, R.A. Soref, P. Payson, S. Johns, and E. N. Toughlian, "Photonic beamformer for phased array antennas using a fiber grating prism," *IEEE Photon. Technol. Lett.*, vol. 9, pp. 241 -243, 1997.

[19]   G. A. Ball, W. W. Morey, and W. H. Glenn, "Standing-wave monomode erbium fiber laser," *IEEE Photon. Technol. Lett.*, vol. 3, pp. 613-115, 1991.

[20]   D. Wei, T. Li, Y. Zhao, et alia, "Multiwavelength erbium-doped fiber ring laser with overlap-written fiber Bragg gratings," *Opt. Lett.*, vol. 25, pp. 1150-1152, (2000).

[21]   S. K. Kim, M. J. Chu, and J. H. Lee, "Wideband multiwavelength erbium-doped fiber ring laser with frequency shifted feedback," *Opt. Commun.*, vol. 190, pp. 291-302, 2001.

MONASH
UNIVERSITY

[22]   Z. Li, L. Caiyun, and G.Yizhi, "A polarization controlled multiwavelength Er-doped fiber laser," presented at APCC/OECC99, 1999.

[23]   R. M. Sova, C. S. Kim, and J. U. Kang, "Tunable dual-wavelength all-PM fiber ring laser," *IEEE Photon. Technol. Lett.*, vol. 14, pp. 287-289, 2002.

[24]   I. D. Miller, D. B. Mortimore, P. Urquhart, et al., " A Nd3+-doped cw fiber laser using all-fiber reflectors," *Appl. Opt.*, vol. 26, pp. 2197-2201, 1987.

[25]   X. Fang, and R. O. Claus, "Polarization-indenendent all-fiber wavelength-division multiplexer based on a Sagnac interferometer," *Opt. Lett.*, vol. 20, pp. 2146-2148, 1995.

[26]   X. Fang, H. Ji, C. T. Aleen, et al., "A compound high-order polarization-independent birefringence filter," *IEEE Photon. Technol. Lett.*, vol. 19, pp. 458-460, 1997.

[27]   X. P. Dong, Li, S., K. S. Chiang et al., "Multiwavelength erbium-doped fibre laser based on a high-birefringence fibre loop," *Electron. Lett.*, vol. 36, pp. 1609-1610, 2000.

[28]   D. Jones, H. Haus, and E. Ippen, "Subpicosecond solitons in an actively mode locked fibre laser," *Opt. Lett.*, pp. 1818-1820., 1996.

[29]   X. Zhang, M. Karlson and P. Andrekson, "Design guideline for actively mode locked fibre ring lasers," *IEEE Photonic tech. Lett.*, pp. 1103-1105, 1998.

[30]   A. E. Siegman, *Laser*. Mill Valley, C.A.:: University Press, 1986.

[31]   J. J. E. Slotine, and W. Li, *Applied Nonlinear Control*. Englewood Cliffs, NJ: Prentice-Hall, 1991.

[32]   E. L. Goldstein, L. Eskilden, V. da Silva, et al., "Inhomogeneously broadened fiber-amplifier cascades for transparent multiwavelength lightwave network," *IEEE J. lightwave Technol.,*, vol. LT-13, pp. 782-790, 1995.

[33]   S. Yamashita, and K. Hotate, "Multiwavelength erbium-doped fibre laser using intracavity etalon and cooled by liquid nitrogen," *Electron. Lett.*, vol. 2, pp. 1298-1299, 1996.

[34]   A. Bellemare, M. Karasek, M. Rochette, S. Lrochelle, and M. Tetu, "Room temperature multifrequency erbium-doped fiber lasers anchored on the ITU frequency grid," *IEEE J. Lightwave Technol.*, vol. 18, pp. 825-831, 2000.

MONASH
UNIVERSITY